Impact of Wind and River Flow on the Timing of the Rivers Inlet Spring Phytoplankton Bloom

by

Megan Amelia Wolfe

B.Sc., The University of British Columbia, 2007

A THESIS SUBMITTED IN PARTIAL FULFILLMENT OF
THE REQUIREMENTS FOR THE DEGREE OF

MASTER OF SCIENCE

in

The Faculty of Graduate Studies

(Oceanography)

THE UNIVERSITY OF BRITISH COLUMBIA

(Vancouver)

July 2010

Abstract

The primary objective of this masters study is to develop an understanding of the physical processes driving the timing of the spring phytoplankton bloom in Rivers Inlet. The spring bloom is initiated as light limitation is lifted causing an increase in growth which overcomes loses due to grazing and advection. The bloom is terminated by nitrate exhaustion. The physical system can impact the spring bloom through variations of winds, cloud coverage, and river input. Strong winds showed two effects. First, strong winds increased the mixing layer depth which decreased the amount of light available for phytoplankton, thus delaying the timing of the spring bloom. Second, large outflow winds caused flushing events to occur resulting in rapid horizontal advection removing the plankton population from the area. River discharge has two opposite effects on the timing of the spring bloom. High river discharge causes the water column to stratify, reducing the mixing layer depth which provides more light available for growth and results in an earlier bloom. High discharge will also result in higher upwelling advection leading to a larger advective loss term for phytoplankton, delaying the bloom. Changes in cloud coverage will directly affect the incoming solar radiation and the light available for photosynthesis.

A coupled bio-physical model is used to explore the driving forces involved in the timing of the spring phytoplankton bloom in Rivers Inlet, British Columbia, Canada. The primary control on the timing of the spring bloom in Rivers Inlet is wind speed and direction. Secondary control on the timing is due to freshwater flow; high river discharge delays the bloom in Rivers Inlet. Single outflow wind events can result in a 7 day delay in the bloom timing. The shift in bloom timing resulting from multiple outflow wind events is greater than the sum of the individual wind events. Implications of flushing events in fjords along the British Columbia coastline are also discussed.

Table of Contents

Appendices

List of Tables

List of Figures

Acknowledgments

I would like to thank my supervisor, Dr. Susan Allen for being the driving force behind my masters thesis. She always had my best interest in mind and helped me achieve my aspirations. Susan, your compassionate and honest nature has kept me grounded and realistic about my goals and has made me strive to become a better scientist.

I would like to thank my committee members, Dr. Brian Hunt, Dr. Evgeny Pakhomov, and Dr. Rich Pawlowicz, for providing consultation, helpful discussions, and insightfulness throughout my thesis work.

This project was a small part of a much larger study which involved many people who made this research possible. Special thanks go out to the sea-techs: Lora Pakhomova and Chris Payne, my fellow graduate students: Asha Ajmani, Jade Shiller, Mike Hodal and Desiree Tommasi, the Rivers Inlet family: Bachen Family, the Western Bounty Crew, and finally the Tula Foundation who has graciously funded the Rivers Inlet Ecosystem Study. I would like to thank Doug Latornell for technical support regarding the SOG model.

I thank my family and friends who have seen me through this journey. Elliot, thank you for your love and support, your countless pep talks and your innate ability to put things into perspective.

Statement of Collaboration

This project was initiated by my supervisor, Dr. Susan Allen. I modified the model developed by Collins et al. (2009) to be used in the Rivers Inlet basin. To utilize the model for my thesis, I required a massive amount of data which was provided by multiple persons including Mike Hodal, Dr. Brian Hunt, Dr. Evgeny Pakhomov, Dr. Rich Pawlowicz, Dr. Rick Routledge and Desiree Tommasi. I ran sensitivity tests to determine the effects of different physical forcings on the timing of the spring phytoplankton bloom. Dr. Allen provided consultation and insight into determining the driving forces on the spring bloom, including the idea and code of flushing events within the inlet. Dr. Hunt and Dr. Pakhomov provided helpful discussions and clarified many of the biological details. Chapter two will be revised into a manuscript co-authored with Dr. Allen, Dr. Pawlowicz, and possible others. Appendix C, which will be an appendix to the manuscript, was co-written by Dr. Susan Allen. As the first author, I was in charge of the literature review, data analysis and preparation of the manuscript with guidance and corrections from Dr. Allen.

Chapter 1

Introduction

This thesis is written as part of the Rivers Inlet Ecosystem Study (RIES), which is a multidisciplinary project involving scientists from the University of British Columbia, Simon Fraser University and the Department of Fisheries and Oceans, Canada. The Rivers Inlet Ecosystem Study was initiated to investigate the driving forces behind the collapse of the Rivers Inlet sockeye salmon run. Strong bottom-up trophic links between phytoplankton, zooplankton and fish yields have been found to occur in southern coastal British Columbia (Ware & Thomson 2005). The primary objective of RIES is therefore to develop an understanding of factors influencing the early life history of Rivers Inlet sockeye salmon (*Oncorhynchus nerka*), with special focus on the link between the physical environment, spring plankton abundance, and sockeye smolt growth and survival.

Fisheries are of global importance and influence economic growth, human welfare, and have effects on marine diversity and ecosystems (Kelleher & Weber 2006). Fluctuations in fisheries have been attributed to habitat alteration, increased predator populations, overfishing, and water pollution (Lajus 2004, Lackey 2009a). Decadal and longer scale regime shifts in marine ecosystems caused by changing climate cycles in turn cause fluctuations in fish stock productivity (Harrison & Parsons 2000). Two sudden regime shifts occurred in the NW Europe marine ecosystem in 1979 and 1988 as a consequence of changing environmental factors (Weijerman et al. 2005). Similar research conducted in the North Pacific identified two climatic regime shifts during the winter of 1976-77 and another in 1989 (Hare & Mantua 2000) indicating a shift in climate-ocean interactions throughout the Northern Hemisphere.

Biological fluctuations have been linked to El Niño (Barber & Chavez 1983) and the North Atlantic Oscillation (Ottersen et al. 2001). Whether there is a causal link between fish population response to oceanographic regime shifts or merely a correlated consequence of other unknown processes is still not fully understood and remains difficult to demonstrate (Platt et al. 2007). It is suggested that fluctuations in physical forcings caused by effects of climate change, will have an impact on phytoplankton, copepod herbivores

and zooplankton carnivores. This will inevitably require fish, seabirds and marine mammals to adapt to a changing spatial and temporal distribution of primary and secondary production (Richardson 2004).

There is significant evidence accumulating that shows trends in Pacific salmon abundance are linked to climate changes (Beamish et al. 1999) as well as evidence of bottom up control of fish production. Apparent instances of bottom up control have been reported in the northeast Pacific Ocean (Ware & Thomson 2005) and Atlantic Ocean (Richardson 2004). Fluctuations in salmon populations have been linked to shifts in primary productivity (Frederiksen et al. 2006, Richardson 2004, Ware & Thomson 2005) and macrozooplankton abundance (Richardson 2008), which in turn can be linked to physical changes in the ocean (Lavaniegos et al. 1998, Richardson 2008, Wiafe et al. 2008).

Rivers Inlet is a temperate coastal fjord located on the central coast of British Columbia, Canada. Historically, Rivers Inlet was the location of one of the largest sockeye salmon runs in Canada. It provided a source of economic stability and a way of life for the Wuikinuxv people, as well as being a major contributor to the commercial fishing industry in British Columbia (Foskett 1958, Godfrey 1958, McKinnell et al. 2001). The sockeye salmon stock began to experience instability in the late 1970's and crashed in the early 1990's, with returns dropping to only 1% of the historical averages (DFO 1997, McKinnell et al. 2001). This collapse of the Rivers Inlet stocks drastically changed the subsistence culture of the aboriginal residents (Rutherford & Wood 2000, McKinnell et al. 2001).

Preliminary findings point to an increased mortality in the early marine stages of the sockeye lifecycle as the source of population decline (McKinnell et al. 2001), possibly due to unfavorable conditions for growth at first marine entry. The spring phytoplankton bloom drives the zooplankton bloom biomass and composition (Richardson 2004, Irigoien et al 2004, El-Sabaawi et al. 2009). Zooplankton are the primary food source of juvenile sockeye salmon (Foerster 1968, Pauley et al. 1989), and thus changes in the timing and composition of these lower trophic levels may be a contributor to fluctuations in sockeye salmon biomass. Tommasi et al. (2010a) hypothesized that higher cloud cover, increased wind events and higher freshwater discharge result in a delayed, short-lived spring bloom. Understanding how the driving physical variables affect the timing and duration of the spring phytoplankton bloom and the effects this will have on sockeye salmon juvenile growth rates through changes in zooplankton will be essential to ecosystem based management under climate change.

While Rivers Inlet has experienced a drastic collapse in the sockeye

salmon stock, this is not an isolated incident. Corresponding declines have been seen in Northern and Central BC (McKinnell et al. 2001, Rutherford & Wood 2000, Riddell 2004). Of the 65 lakes that could be assessed in the central and north coastal regions, 34% were categorized as depressed, indicating they were less than 25% of their base abundance (Riddell 2004). Pacific salmon stocks along the West Coast of Canada have been in sharp decline since the early 1990's (Noakes et al. 2000). In 1993, the National Marine Fisheries Service initiated a status review of coho salmon in Washington, Oregon, and California in response to petitions seeking protection for coho salmon under the Endangered Species Act. It was determined that the natural populations of coho salmon along the California coast were in danger of extinction, while populations along the Washington and Oregon coast lines were likely to become endangered in the foreseeable future (Weitkamp et al. 1995). Noakes et al. (2000) reasoned that the most likely causes for the decline in Pacific salmon stocks were a combination of overfishing, climate change and freshwater habitat destruction. Large-scale salmon enhancement projects have been in place to help curtail the declining salmon populations (Lackey 2009b). Despite the continued release of millions of hatchery salmon, the survival rates of Pacific salmon in the Strait of Georgia rapidly declined in the 1990's. Pacific salmon are a complicated natural resource along the west coast of North America with many regional stocks being driven to near extinction (Lackey 2009b). Further research is needed to understand the underlying causation of the decline in Pacific salmon and to provide valuable information to current policy makers.

To examine how fish populations are affected by fluctuations in primary productivity and climate cycles, it is important to investigate the physical factors affecting the growth of phytoplankton on an appropriate regional scale. Studies have shown that juvenile salmon survival rates co-vary within the order of 100 to 1000km (Mueter et al. 2002). This implies that only regional factors are important in the survival rates of juvenile salmon. The coastal regions of British Columbia are important staging areas for juvenile salmon and while the importance of bottom up control is becoming more evident, the physical variables driving phytoplankton production in temperate coastal fjords is still not well understood (Tommasi et al. 2010a).

Phytoplankton abundance is largely controlled by nutrients, light availability, advection and temperature of the water column (Reynolds 2006, Winter et al. 1975). In temperate regions, there is a strong seasonal cycle of nutrients and light. Sverdrup (1953) proposed a model in which changes in the mixed layer depth affect the timing of the spring bloom. During the winter season, strong winds mix nutrients up into the surface layer and a deep

mixed layer is formed. Light availability is the limiting factor in phytoplankton growth. The phytoplankton are mixed below their critical depth, the mixing depth at which the water column integrated photosynthesis equals the water column integrated respiration, and are not able to grow. As the days become longer, incoming radiation increases, and thus the critical depth deepens. Winds decrease and incoming solar radiation heats the upper water column, both decreasing the mixed layer depth and increasing stratification in the water column. A sudden burst of phytoplankton biomass, termed a spring bloom, will occur when the critical depth equals the mixed layer depth (Longhurst 1995). Nutrients now become the limiting growth factor. During the summer months, nutrients cannot be replenished from deeper waters due to the increase in water column stratification. Blooms collapse when the limiting nutrient has been exhausted in the euphotic zone. Phytoplankton growth rates are tightly correlated to nutrients, temperature and light availability for photosynthesis. Changes in these variables would affect the spatial extent and timing of the phytoplankton blooms (Tommasi 2008).

The classic Sverdrup model for phytoplankton dynamics has been well developed and validated with observations from many situations including estuaries and in coastal upwelling areas (Mann & Lazier 2006). However, the influence of the mixed layer depth may be of less importance in a variety of other marine environments (Lucas et al. 1998, Huisman et al. 1999). In the Strait of Georgia, mixing occurs without homogenizing the temperature or salinity due to a significant buoyancy flux into the upper water column (Collins et al. 2009). This mixing layer, the layer that is actively mixing, must be distinguished from a mixed layer, which is defined as a region near the surface that is well mixed with respect to temperature and salinity (Collins et al. 2009). Following Large et al. (1994) we use the definition that the mixing layer depth is the depth to which the bulk Richardson number remains less than 0.3, such that, below this depth stratification inhibits surface forced turbulence. An influx of freshwater can result in a mixed layer depth that is shallower than the critical depth, but due to a mixing layer that is deeper than the critical depth, phytoplankton growth is inhibited. This effect has been seen in other regions where it has been assumed that mixing is occurring down to a strong halocline (Erga & Heimdal 1984). Other deviations from the Sverdrup model include spring blooms that were observed to occur in Norwegian fjords in the absence of a mixed layer (Eilertsen 1993) as well as in the Gulf of Maine (Townsend et al. 1992). Another limiting factor for phytoplankton growth is advective loss (Winter et al. 1975). Wind-driven advection causing the removal of a plankton population from a basin has been observed in Puget Sound (Winter et al. 1975)

and in Otsuchi Bay, Japan (Furuya et al. 1993).

The primary objective of the work reported here is to develop an understanding of the driving forces of the spring phytoplankton bloom. I examined the environmental variables helping to initiate and drive the spring phytoplankton bloom within Rivers Inlet using a coupled biophysical model (SOG) originally developed to predict the spring bloom in the Strait of Georgia. The physical model is a one-dimensional, vertical-mixing boundary layer model (Large et al. 1994), while the biological model uses one class of phytoplankton and uses nitrate as the sole nutrient to determine growth rates (e.g. Dickson and Wheeler, 1995). The biophysical model requires local forcings including air temperature, wind, clouds, humidity, river outflow and nutrient levels. Sources of historical meteorological data are not present for Rivers Inlet, requiring an examination of longterm meteorological data from surrounding areas (e.g. Port Hardy) to compare to short term in-situ measurements to allow extrapolation to simulate the conditions for Rivers Inlet. Higher vertical resolution (0.25m) was needed to correctly model the shallow freshwater layer observed in Rivers Inlet. A one-sided open basin system was developed to correctly depict the bio-physical dynamics occurring within Rivers Inlet during outflow wind events. The physical model is used to reproduce the mixing due to turbulent vertical velocities of unresolved eddies and numerically calculates horizontal velocities, temperature, salinity, and diffusivities in both space and time.

The SOG model incorporated many processes in addition to the original KPP mixing model to adapt to a coastal region (Collins et al. 2009). Modifications to some of these additional parametrizations in the SOG model were made to use the model in the Rivers Inlet basin. In-situ measurements of temperature, salinity and nitrate averaged from 40-50m were used to calculate an empirical fit to constant and seasonal components used as bottom boundary conditions for the model.

Estuarine circulation has two effects which must be accounted for in Rivers Inlet. First, the influx of freshwater into the surface layer of Rivers Inlet causes it to remain relatively fresh and keeps the water column stratified. This required a parametrization of the effects of freshwater specific to Rivers Inlet and the input from Wannock River. Second, vertical advection is affected by estuarine entrainment, and a parametrization to determine the influence of freshwater inflow on estuarine entrainment processes was developed. A parametrization for the absorption of light in the water column was calculated to specify the light conditions for River Inlet.

This study eludicates the physical controls that are driving the timing of the spring phytoplankton bloom in Rivers Inlet and demonstrates how large

variations in environmental variables can cause considerable differences in the timing of the spring bloom. Wind speed and direction are the primary control of the timing of the spring bloom. Sustained outflow wind events will result in basin flushing. Rapid horizontal advection of the phytoplankton population out of the basin delays the onset of the bloom. Large outflow wind events are observed in Rivers Inlet and Burke Channel leading up to the spring bloom. This suggests the importance of flushing events to the spring bloom timing along the British Columbia coastline. Climatic changes in the large scale low pressure systems that drive the outflow wind events along the coastline would potentially cause changes in the frequency and occurrence of outflow events and ultimately change the timing of the spring phytoplankton bloom. The timing of the spring bloom may be influential in the survival of higher trophic levels (Cushing 1974, 1975, 1982, Richardson 2004, Ware & Thomson 2005). Possible match/mismatch of the phytoplankton bloom and higher trophic levels could have led to the decline of the sockeye salmon in Rivers Inlet. This research brings new insight into the physical controls of the primary productivity in fjords and in particular Rivers Inlet and will hopefully answer some of the questions that the Rivers Inlet Ecosystem Study set out to address about the decline of sockeye salmon in Rivers Inlet.

Chapter 2

Impact of advection loss due to wind and estuarine circulation on the timing of the spring phytoplankton bloom in a British Columbia fjord

2.1 Introduction

In temperate regions, phytoplankton follow a strong seasonal cycle which is typically characterized by a prominent spring phytoplankton bloom. The spring bloom occurs when growth rates of phytoplankton exceed the loss rates from a variety of processes, resulting in a rapid accumulation of biomass (Longhurst 1995). Growth rates of phytoplankton are determined by light and nutrient limitations and can be mediated by water temperature (Parsons et al. 1984, Reynolds 2006). Light and nutrient levels in turn are strongly affected by physical processes.

Sverdrup (1953) proposed a model in which physical processes affect the timing of the spring bloom by varying the mixed layer depth. While the classical critical depth theory has been well developed and validated with observations in many situations including estuaries and in coastal upwelling areas (Mann & Lazier 2006), the influence of the mixed layer depth may be of less importance in other marine environments (Lucas et al. 1998, Huisman et al. 1999). A model of the spring bloom in shallow estuaries found that leakage of phytoplankton from the shallow surface layer as well as sinking or turbulent diffusion in permanently stratified estuaries is important and must be taken into consideration when modeling the spring bloom (Lucas et al. 1998). Flushing events have been seen in Puget Sound (Winter et al.

1975) and in Otsuchi Bay, Japan (Furuya et al. 1993) where sustained winds have resulted in rapid horizontal advection causing an exchange in water masses which dilute the phytoplankton populations in the basins. Other factors affecting biomass accumulation are grazing, sinking, advection and viral lysis (Welschmeyer & Lorenzen 1985, Collins et al. 2009).

British Columbia is well known for its complex coastline, interwoven with fjords and inlets. Fjords are associated with high latitudes and glacial activity. They are characterized by steep sides and deep, elongated channels with a sill (Pedersen 1978, Valle-Levinson 2010). A significant loss term in many fjord regions is dilution due to vertical entrainment, a result of estuarine circulation and wind-driven advection (Lucas et al. 1998). The strength of the estuarine circulation is determined by the freshwater flux into the fjord. Fjord estuarine circulation is characterized by moderate to large river discharge and a weak to moderate tidal forcing resulting in a strongly stratified estuary (Pedersen 1978, Valle-Levinson 2010). A shallow surface layer transports freshwater out towards the inlet mouth while deeper and often nutrient-rich waters enter the inlet over the sill at the mouth of the fjord. Phytoplankton located in the freshwater-driven current will experience horizontal advection with estuarine circulation controlling the horizontal distribution of the plankton (Kaartvedt & Svendsen 1990). In coastal embayments, large wind events can also result in rapid horizontal advection, flushing the phytoplankton population out of the area (Winter et al. 1975). Sustained winds large enough to reverse the surface layer flow were found to occur in Knight Inlet, a British Columbia fjord (Baker & Pond 1995).

Poor understanding of the physical forcing variables of phytoplankton production and the potential contribution to the decrease in marine survival rates of juvenile salmon warrants study of the driving forces that effect the timing of the spring phytoplankton bloom. In this paper, a numerical model is used to analyze the impact of advective loss due to wind and estuarine circulation on the timing of the spring bloom in a British Columbia fjord. Rivers Inlet fjord is the system being modelled. Rivers Inlet is a temperate coastal fjord, located on the central coast of British Columbia (Figure 2.1), that historically hosted one of the largest sockeye salmon runs in Canada until stocks collapsed in the 1990's. The inlet is uniformly deep (200-300 m), is 40 km long and 3 km wide, and has a relatively deep and complex sill region at its mouth (depth 110 m), opening into Queen Charlotte Sound. The major source of freshwater is the Wannock River located at the head of the Inlet which drains Oweekeno Lake.

There is considerable interannual variability in the timing and duration

of the spring bloom in Rivers Inlet (Tommasi et al. 2010a). In other regions it has been suggested that the timing of the spring bloom may be influential to the survival of various higher trophic levels through a match/mismatch process (Cushing 1974, 1975). For example, in the Strait of Georgia, early spring blooms can cause nauplii of *N. plumchrus*, which migrate to the surface in the spring, to miss the spring bloom causing them to rely solely on post-bloom phytoplankton which are less abundant and less nutritious (El-Sabaawi et al. 2009). In Rivers Inlet, a late spring bloom resulted in a smaller, delayed zooplankton biomass peak and a change in the zooplankton community composition (Tommasi et al. 2010a). Zooplankton are the primary food source of juvenile sockeye salmon (Foerster 1968, Pauley et al. 1989), and thus changes in the timing and composition of these lower trophic levels may be a contributor to fluctuations in sockeye salmon biomass.

In Rivers Inlet, we expect the interannual variation in the timing of the spring bloom to be dependent on mixing layer depth, advective loss, and incoming radiation. Nutrient availability should not be a factor in determining the onset of the bloom, although it influences the termination of the bloom. Winter concentrations of zooplankton are similar between years and concentrations do not increase significantly until after the spring phytoplankton bloom occurs (Tommasi et al. 2010a). Thus zooplankton grazing has an insignificant effect on the interannual variation of the timing of the spring phytoplankton bloom. We use a coupled bio-physical model (Collins et al. 2009) to determine which physical forcings most strongly influence the timing of the spring phytoplankton bloom in Rivers Inlet. A quasi one-dimensional vertical mixing model is used to model the physical properties of Rivers Inlet . The physical model is a K-Profile Parametrization (KPP) non-local boundary layer model (Large et al. 1994) adapted to a coastal fjord region (Collins et al. 2009). The model reproduces the mixing due to turbulent vertical velocities of unresolved eddies and numerically calculates horizontal velocities, temperature, salinity, and diffusivities in both space and time. To carefully determine the effects of surface mixing on phytoplankton growth, fine vertical resolution is needed. Here we use a vertical resolution of 0.25m to resolve the near-surface mixing processes and to correctly depict the spring phytoplankton bloom. In Rivers Inlet, the initial spring bloom occurs near the surface with the chlorophyll maximum occurring above 3 meters. This resolution is easily achieved in a 1-D model, but would be very difficult in a 2-D or 3-D model. Knowledge from previous studies and high resolution data being collected allow us to parametrize the necessary 2D physical processes (estuarine circulation, baroclinic pressure gradients) and tune the 1D model to correctly represent the Rivers Inlet

physical processes.

The spring bloom is initiated as light limitation is lifted and, in Rivers Inlet, is terminated by nitrate exhaustion. The first organisms to bloom are diatoms, primarily *Thalassiosira* spp (Tommasi et al. 2010a). Our model is thus limited to one nutrient type (nitrate) and one phytoplankton class (diatom). This model is fast and simple, allowing for both an interpolative mode for the years with observed data, and an extrapolative mode for years where data does not exist and for hypothetical forcings. This will allow us to be able to vary the physical forcings (wind speed, cloud coverage, and freshwater flux) to determine the individual impacts on the timing of the spring bloom. The following sections will discuss the observational data needed to initialize and force the model, the physical model and biological model (Section 2.2), model results (Section 2.3), discussion to address which physical processes are affecting the initiation of the spring phytoplankton bloom in Rivers Inlet and the significance to other fjord regions (Section 2.4).

2.2 Data and Methods

2.2.1 Data

The field data used in this research was collected for the Rivers Inlet Ecosystem Study during the early spring and summer months of 2007, 2008 and 2009. Sampling took place approximately twice monthly between February and August (Tommasi et al. 2010a, Hodal & Pawlowicz 2010). The station chosen to be modeled is DF02 (Figure 2.1). In 2007 and 2008, daily sampling of temperature, salinity, photosynthetically active radiation (PAR) and chlorophyll fluorescence took place at the Florence Daily site located near DF02 down to 30 m using a Hydrolab®DS5X sonde. During the 2008 season, the Hydrolab®sonde broke down several times. For the periods April 1 to April 9th, April 30 to May 15, May 25 and 26, June 8, and June 14 to 22, 2008, profiles of temperature, salinity and fluorescence were taken using a SBE 25 Sealogger CTD (Tommasi et al. 2010a). In 2009, the daily profiles were taken using a RBR XR-620 CTD. During the twice monthly cruises, profiles of temperature, salinity, chlorophyll fluorescence, and PAR were taken using the SBE25 CTD. Nitrate, phytoplankton, and chlorophyll a were sampled using Niskin bottles at depths 0 m, 5 m, 10 m, and 30 m.

Meteorological field data was obtained from 2 weather stations that were mounted near DF02 (Figure 2.1) (R. Routledge, personal communication, February 21, 2009, Hodal & Pawlowicz 2010) and from the Port Hardy

meteorological station (Environment Canada 2009). Laska weather station replaced Ethel weather station in 2009. Hourly values of wind speed and direction were collected from Ethel and Laska station during March and April of 2008 and 2009. Data collected from the Port Hardy meteorological station included daily values of humidity, cloud fraction data, air temperature, and hourly wind speed and direction. Daily Wannock River discharge data was obtained from the Water Survey of Canada (Environment Canada 2006).

2.2.2 SOG Model

The SOG model is a one-dimensional coupled biophysical model. It successfully predicts the timing of the spring phytoplankton bloom in the Strait of Georgia, British Columbia, Canada (Collins et al. 2009). Details of the model are given in Appendix A and B. The model is initialized using a fall profile of temperature (T), salinity (S), chlorophyll fluorescence and nitrate (M. Robert, unpublished data, 2005-2007. IOS/OSD Data Archive: DFO, Hodal & Pawlowicz 2010). The biology model is optimized to predict the interannual variation in the timing of the spring bloom from 2007-2009.

2.2.3 Physical Model Modifications

The physical model is tuned to provide realistic parameters to describe the physical dynamics of the Rivers Inlet system. The tuned physics model is coupled with the biology model which is then tuned independently to correctly match the timing of the spring phytoplankton bloom. The physical model incorporates many additional processes to the original KPP mixing model to adapt to a coastal region (Collins et al. 2009). Modifications to these additional parametrizations in the SOG model were made to to use the model in the Rivers Inlet basin.

At this point, it is useful to distinguish between variables estimated from observations and tuned variables. There are numerous parametrizations used in the model in which a variable is determined from observational data of some kind and not tuned thereafter. A tuned variable, on the other hand, is one that is used in the model and is adjusted to produce the most favorable model output. Parametrizations of variables estimated from observations are discussed in the following subsections, while tuning variables are described in Sections 2.3.1 and 2.3.2.

Estuarine Flow

Estuarine circulation has two effects. First, the influx of freshwater into the surface layer of a fjord causes it to remain relatively fresh and keeps the water column stratified. Second, vertical advection is assumed to be largely controlled by estuarine entrainment.

Freshwater is added into the surface layer based on a parametrization of total freshwater flow into the Inlet. The surface salinity at station DF02 is observed to be correlated with the Wannock River flux. An empirical fit is:

$$S_{surface} = S_D \frac{\exp\left(-Q_W/\alpha_1\right) + \beta \exp\left(-Q_W/\alpha_2\right)}{\gamma_1 + \exp\left(-Q_W/\alpha_1\right) + \beta \exp\left(-Q_W/\alpha_2\right)} \tag{2.1}$$

where Q_W is the Wannock River flux, $S_D = 31.8$, the observed average salinity between 40-50 m in Rivers Inlet, $\alpha_1 = 80.0$ m^{3}s^{-1}, $\alpha_2 = 1500.0$ m^{3}s^{-1}, $\gamma_1 = 0.04$, $\beta = 0.01$ (Figure A.1). The surface salinities of the model are then forced this fit using the following dilution rate to decrease salinities:

$$J_s \exp(\gamma z) = F_w Q_W S_o \left(\frac{Q_W}{\overline{Q}}\right)^{\sigma_s} \exp\left(\frac{z}{a_h h_m}\right) \tag{2.2}$$

where $F_w = 2.0\text{x}10^{-6}\text{s}^{-1}$, S_o is the mixed layer salinity at the previous time step, $a_h = 3.5$, $\overline{Q} = 7000$ m^{3}s^{-1}, $\sigma_s = 1.38$, z is vertically upward starting at the sea surface, and h_m is the mixing layer depth determined by the KPP model. The constants F_w, σ_s, and a_h were tuned to match the model surface salinity to the interpolated observed salinity (see Section 2.3.1). To determine a good match between model and observed halocline depths, the depth over which freshwater was added (a_h in equation 2.2) was tuned.

Estuarine entrainment largely controls upwelling in a fjord and is also parametrized in the model. The magnitude of the vertical velocity as a function of Wannock River flow was determined using the Knudsen Relations (Dyer 1973) based on salinity observations at DF02 assuming a 16 m deep surface layer. Its vertical profile was determined using a force balance between the estuarine pressure gradient and turbulent momentum mixing (Collins et al. 2009). To relate upwelling velocity to river discharge we use:

$$w_e = w_* \left[\frac{Q_W}{\overline{Q}} \exp\left(\frac{-Q_W}{\overline{Q}}\right)\right] \left[1 - \left(1 - \frac{z}{2.5d}\right)^2\right] \tag{2.3}$$

where $w_* = 1.08\text{x}10^{-4}\text{ms}^{-1}$ and $d = 6.4$ m is the average depth at which the cumulative freshwater reaches 67% of its total value at DF02. For the flow rates observed for the Wannock River ($<3000\text{m}^3\text{s}^{-1}$), equation 2.3 is

nearly linear in Q_W; we include the exponential term to give model stability for hypothetical very large river flows. This vertical velocity advects temperature, salt, momentum, nitrate and phytoplankton in the model. The vertical velocity is strongest at depth compared with the surface causing a vertical convergence of water which results in a horizontal removal of these properties throughout the depth of the modeled water column.

Wind-driven Vertical Advection

The Strait of Georgia was modeled as a closed basin system (Collins et al. 2009) but advection out of the mouth of Rivers Inlet due to outflow winds is an important loss mechanism. A one-sided open basin system was developed to correctly depict the bio-physical dynamics occurring within a fjord during outflow winds. During an outflow wind event, the mouth of the fjord is assumed to have an outflow velocity equal to the velocity seen at the central, modelled station. This causes the surface layer to flow out of the inlet, resulting in deeper water moving upwards to replace it. Upwelling occurs requiring the additional parametrization of a wind driven vertical velocity which was added to the entrainment velocity, w_e. Vertical advection is thus being driven by both estuarine circulation and wind. Details of the one-sided open basin system can be found in Appendix C.

Internal Mixing

Rivers Inlet is much narrower than the Strait of Georgia. When numerically calculated, the baroclinic velocities produce high vertical mode numbers leading to step-like mixing which is not seen in the observations. To remove this unrealistic behavior, the model was forced to have stronger implicit mixing by smoothing the diffusivity calculated by the model over 5 grid points rather than the 3 grid points used in Collins et al. (2009).

Light

The SOG physical model incorporates light in 3 parts: a cloud model (which determines the amount of light penetrating the atmosphere at a given time and hitting the water surface), an albedo (which controls how much light enters the water column), and the parametrization for the depth profiles of photosynthetically active radiation, I_{par}, and the total light spectrum that is available for heating, I_{total}. The total non-reflected light entering the water column, $I_{total}(0m)$, is calculated by the geometry of the solar angle for a given time and latitude and the cloud filtering (Collins et al. 2009).

The profiles of I_{total} with depth is based on the Jerlov (1976) classification (Collins et al. 2009).

To specify the light conditions in the water column, a photosynthetically active irradiance profile must be determined through a parametrization of the attenuation coefficient, K_{par}. Examination of I_{par} profiles taken at the daily station from February - June 2009 (Hodal & Pawlowicz 2010) showed a positive correlation between the attenuation coefficient and with the amount of phytoplankton mass in the water column (based on chlorophyll concentrations) and no significant correlation with river discharge. River turbidity is not significant until after the freshet begins, which occurs after the spring bloom (R. Pawlowicz, personal communication, December 4, 2009). I_{par} profiles measured in 2007 with another instrument were apparently too dark to sustain a phytoplankton population and were deemed unreliable. Data from other years was unavailable. An empirical fit of the change in I_{par} over depth, eK, was determined where $eK = \exp(-K_{par}dz)$ is a function of depth with $dz = 1$m. The empirical relationship between the measured light and the phytoplankton quantity in the water (measured chlorophyll, P_c) was found to be:

$$K_{par} = \alpha_l + \beta_l \bar{P}^{0.665} + \theta_l \exp\left(\frac{z}{d_l}\right) \tag{2.4}$$

where $\overline{P} = P_c/(1\text{mg Chl } m^{-3})$ and the exponent on $\overline{P}$ follows Ménesguen et al. (1995). The empirical fit gave $\alpha_l = 0.1709\text{m}^{-1}$, $\beta_l = 0.02\text{m}^{-1}$, $\theta_l = 2.53\ \text{m}^{-1}$, and $d_l = 0.53$m (See Appendix A for details).

Wind

Wind speed and direction measurements come from Port Hardy Airport and the Ethel and Laska weather stations in Rivers Inlet (Environment Canada 2009, R. Routledge, personal communication, February 21, 2009, Hodal & Pawlowicz 2010, respectively). Sources of historical meteorological data are not available for Rivers Inlet. A comparison of nearby longterm meteorological data from surrounding areas with short term in-situ measurements allowed for extrapolation to simulate the conditions for Rivers Inlet. To represent the local wind direction in Rivers Inlet, a regression tree was developed using a comparison between the Port Hardy Airport and the Laska Meteorological Station wind directions (Table 2.1). Wind speed from Port Hardy is used as a proxy for the wind speed in Rivers Inlet. The linear relationship is:

$$V_{RI} = mV_P \tag{2.5}$$

where V_{RI} is the wind speed at Laska weather station, V_P is the wind speed at Port Hardy meteorological station and $m = 0.877$. Wind speed and direction are transformed into meridional and zonal components and rotated to align with the major axis of Rivers Inlet. Wind speed and direction that are available in 2008 and 2009 from Ethel and Laska meteorological stations are used in place of the extrapolated Port Hardy data. Data was available from Ethel station from February 35, 2008 to September 21, 2008. Data from the Laska station was available from March 1, 2009 to April 8, 2009 and June 1,2009 to March 18, 2010. Wind direction from Ethel station was originally calibrated to magnetic north. The wind direction was rotated 19.15° west to calibrate to true north. The wind stresses were calculated from these velocities following Large & Pond (1982).

Bottom Boundaries

Temperatures and salinities from the 2008-2009 Rivers Inlet Ecosystem Study cruises (Hodal & Pawlowicz 2010) were used to determine an annual fit for the bottom boundary inputs. Measurements were averaged between 40-50 m and an empirical fit was determined using a constant and seasonal component. For temperature:

$$T_B = y_1 + y_2 \sin(\omega t + y_3) \tag{2.6}$$

where T_B is the temperature at 40 m, $y_1 = 7.63°\text{C}$, $y_2 = 0.63°\text{C}$, $y_3 = 3.04$, $\omega = 2\pi/365.25\text{day}^{-1}$, and t is the time in yearday. For salinity:

$$S_B = y_1 + y_2 \sin(\omega t + y_3) \tag{2.7}$$

where S_B is the salinity at 40 m, $y_1 = 31.66$, $y_2 = 0.46$, and $y_3 = 4.51$. A 40 m bottom nitrate value of 21μM was calculated by samples taken from bottles during the August 2006, 2007 and 2008 CCGS J.P Tully cruises (M. Robert, unpublished data, 2005-2007. IOS/OSD Data Archive: DFO), along with samples obtained from the 2008 Rivers Inlet fortnightly cruises (Hodal & Pawlowicz 2010). A weighted average nitrate profile was determined for DF02 to initialize the model because the accuracy of the Tully data was higher than that of the Rivers Inlet nitrate data. A weighted mean was calculated for each bottle depth (0, 5, 10, 30, and 50m) using

$$\bar{N} = \frac{\sum_{i=1}^{n} (N_i/\sigma_i^2)}{\sum_{i=1}^{n} (1/\sigma_i^2)} \tag{2.8}$$

where $\bar{N}$ is the weighted nitrate mean at a particular depth, N_i is nitrate measurements, and σ_i is the variance of the measurements for Tully or Rivers

Inlet data. Nitrate concentrations were considered constant at 40m which is consistent with observations seen at multiple stations throughout Rivers Inlet. A low-level constant background value of phytoplankton was used for the bottom boundary inputs.

2.2.4 Biological Model Modifications

The primary objective of the biological component of the SOG model, when coupled with the physical model, is to predict the timing of the spring phytoplankton bloom. A simple model is used to determine the growth rate of phytoplankton. As light limitation is lifted, a spring bloom is initiated which is then terminated by nitrate exhaustion, the limiting nutrient in Rivers Inlet (Figure 2.2). Only one size class of phytoplankton is used (microphytoplankton, $>20\mu$m) and only nitrate is modeled as a nutrient. During the spring bloom, over 99% of the total phytoplankton abundance is diatoms. In 2007, the bloom contained both *Skeletonema costatum* and *Thalassiosira* spp. (Tommasi et al. 2010a). A phytoplankton analysis was done on samples taken from 10m at DF02 during 2 cruises dating March 31, 2008 and April 23, 2008. *Thalassiosira spp.* was found to bloom first in Rivers Inlet in 2008. In the model, we use *Thalassiosira* spp.. Modeling *Skeletonema costatum* instead of *Thalassiosira* spp. would cause an insignificant difference in finding the timing of the spring bloom because both diatoms have high growth rates at low light and low temperatures. While ammonium is being used by phytoplankton, the amount of ammonium available at any time is too small to sustain the biomass of the spring bloom for longer than several hours, and its inclusion in the model was shown to make no substantial changes to the spring bloom timing (Collins et al. 2009).

Phytoplankton concentrations are affected by growth rates, natural mortality, grazing, sinking and physical processes. Growth rates are based on light and nutrient limitation. Growth rates, grazing and mortality are dependent on temperature. Grazing is based on a tuned concentration of zooplankton that is held constant. Winter concentrations of zooplankton in Rivers Inlet are similar between years (Tommasi et al. 2010a). Zooplankton concentrations do not increase significantly until after the spring phytoplankton bloom occurs (Tommasi et al. 2010a), allowing for a constant zooplankton concentration to be used in a model to determine the timing of the spring bloom. A density-dependent mortality rate was used to described the functional response of zooplankton grazing at very low chlorophyll levels. The grazing threshold is defined as the concentration of prey, below which, the predator stops feeding (Cugier et al. 2005, Leising et al. 2003). A

value of 0.09mg Chl/m^{-3} was used for the chlorophyll predation threshold. The physical processes include loss due to entrainment and turbulent diffusion determined by the physical model. Advective terms due to horizontal variations in phytoplankton concentration are not included in the model. The timing of the spring bloom is nearly spatially uniform in the inlet with differences in bloom timing at different sites a maximum of three days apart (Tommasi et al. 2010a). Table 2.2 gives values for all biological parameters modified from Collins et al. (2009).

2.3 Results

2.3.1 Physical Model Tuning

The physical model was run independently of the biological model and compared with observations. The model was deemed useful when the modeled physical profiles resembled the observed physical profiles. Surface salinity values, and depth and steepness of the halocline were quantitatively compared. The modelled average depth and steepness of the halocline was within one-half of one standard deviation from observations. To modify the physical model, internal mixing and freshwater parameters were tuned. The vertical advection velocity determined through w_* was based on analytic calculations and was not tuned. The internal wave mixing values were set to those used in the Strait of Georgia (Collins et al. 2009). The dilution rate (F_w and σ_s in equation 2.2) was tuned to produce surface salinities that matched the empirical relationship (equation 2.1). The depth range in which freshwater was added (a_h in equation 2.2) was tuned to obtain a good match between the model and observed halocline depth.

2.3.2 Biological Model Tuning

The biological model was tuned independently of the physical model. Two biological parameters were tuned to provide the best match between the timing of the peak magnitude of the modeled spring bloom and the observed spring bloom for the years 2006-2009: maximum growth rate ($R_{max}(T_{ref})$) and concentration of zooplankton (Z_w). The 0-3 m averaged phytoplankton concentrations were compared with daily chlorophyll fluorescence measurements for each model run and surface nitrate was compared to discrete bottle sampled nitrate at 0 m (Figure 2.3). The chlorophyll fluorescence measurements were calibrated to 0.7μm filtered chlorophyll a. Averaged 0-3 m phytoplankton concentration was used because the initial spring bloom

is surface focused with the observed chlorophyll maximum occurring above 3 m in the water column. The spring bloom peak was defined as the date of the maximum 0-3 m averaged phytoplankton concentration within 4 days of the 0-3 m averaged nitrate concentrations going below 0.1μM.

2.3.3 Spring Bloom Timing

The interannual variation in the timing of the spring phytoplankton bloom is predicted successfully with the modeled peaks occurring within +/- 4 days of the observed blooms (Figure 2.3). Considerable interannual variability was seen in the timing of the spring bloom at DF02. The earliest bloom occurs in 2008, with observed 0-3m averaged chlorophyll values peaking on April 3rd. The latest bloom occurs in 2007, on April 28th, as a result of high river discharge and larger, more frequent wind events (Figure 2.4). Blooms in 2008 and 2009 are observed to occur 10 days apart even though wind speed, river flow, cloud coverage, and winter zooplankton abundance are similar between years. As will be shown later (Section 2.4), differences in the wind direction of large wind events occurring within 6 weeks of the initiation of the bloom for 2008 and 2009 appear to have significant effects on the timing of the spring bloom. Initial hindcasts of 2006 using Port Hardy winds extrapolated to simulate the conditions for Rivers Inlet resulted in a spring bloom that occurred on April 30th, 2006. The observed spring bloom occurred between March 29th-April 12th, 2006 (Tommasi 2008). Extrapolating wind direction from Port Hardy to simulate conditions in Rivers Inlet was not precise and resulted in possible error in wind direction even for strong wind events. Reversing the direction of large outflow wind events 6 weeks prior to the 2006 spring bloom (Section 2.3.4) resulted in a bloom occurring on April 11th, within range of observations.

To quantify the effect of different physical forcings on the initiation of the spring bloom, a series of 48 tests was done (Table 2.3). In each test, one physical variable (wind (w), Wannock River flow (r), or cloud coverage (c)) was replaced with data from another time period, while all other variables remained constant. For example, "R6wR7" is the 2006 spring bloom, initialized in September 2005 and run until November 2006 using data from 2005-2006 with the exception of wind data, which was replaced with winds from 2006-2007. Each test scenario was compared to its control year, for example the timing of the R6wR7 bloom would be compared to the 2006 bloom date using 2006 meteorological data. Results of the sensitivity tests are given in Table 2.4 and are described below.

2.3.4 Effect of Winds

The timing of the spring bloom is highly sensitive to the wind speed and direction. Wind events were stronger and occurred more frequently in 2007 than in other years which resulted in a delay in bloom timing for all years run with 2007 wind data. The largest delay of 10 days occurred during the 2006 spring bloom (R6wR7). Wind strength and frequency was similar between 2008 and 2009. Differences in wind direction resulted in delays in the spring bloom for 2006 and 2008 using wind data from 2009, whereas wind data from 2008 with fewer outflow winds, caused an earlier bloom to occur in 2006 and 2009 (Table 2.4).

Sensitivity to Basin Flushing

To explore the sensitivity of the model to wind direction a test case model was run where large outflow winds in 2006 were reversed in direction to flow up inlet (Figure 2.5). Outflow winds to be reversed were selected by having wind speed cubed values over $400 m^3 s^{-3}$ between January 1st and April 28th, 2006. These strong winds grouped naturally into 5 events, each of less than 6 days duration. The original 2006 run using the correlated wind speed and direction from Port Hardy resulted in a spring bloom occurring on April 28th, 2006. All the wind events but one were changed in direction to inflow to determine the effect of single outflow events on the timing of the spring bloom (Table 2.5). Then test runs were done with multiple outflow wind events (Table 2.5). Reversing all 5 wind events to outflow winds produced a bloom that occurred on April 9th, 2006, a 19 day shift. Outflow wind events that occurred in January resulted in a 1 to 2 day shift in the spring bloom timing. Outflow events that occurred in March resulted in a shift of 4 days and events occurring in April shifted the bloom by up to 7 days. Strength of a wind event did not have as strong an effect on bloom timing. Doubling the wind strength of an outflow event 3 weeks prior to the bloom resulted in a 2 day delay in the spring bloom.

2.3.5 Effect of Wannock River Flow

The timing of the spring bloom is sensitive to freshwater flux. Average Wannock River discharge from February through April was stronger in 2007 (226 $m^3 s^{-1}$) compared with 2006 (95 $m^3 s^{-1}$), 2008 (100 $m^3 s^{-1}$) and 2009 (76 $m^3 s^{-1}$). This resulted in all modeled test runs computed with 2007 river data to experience a delayed bloom. Freshwater discharge was similar

in 2006, 2008, and 2009 and there was minimum variation in bloom timing when compared to control years.

River flux has two effects that have opposite effects on the bloom timing. First, higher river discharge causes the water column to become more stratified, resulting in an earlier spring bloom. Second, large river discharge also causes higher upwelling advection leading to a larger advective loss term for phytoplankton, delaying the spring bloom (refer to Appendix A, Freshwater Flux). A sensitivity test was run to determine which river effect was dominant in Rivers Inlet. 2006 was used as the run year for the test case. Constant river discharge was used between January 1, 2006 - April 30, 2006 while observed river discharge values were used the rest of the year. Sixteen test cases were run, starting with a constant discharge of 50 m^3s^{-1} and increasing in increments of 10 m^3s^{-1}, to finish with a constant discharge of 200 m^3s^{-1}. A moderate river discharge of 105 m^3s^{-1} resulted in a spring bloom that occurred on April 22, 2006. At low river discharge (50 m^3s^{-1}), the spring bloom was delayed by 5 days due to a deeper mixing layer depth. High river discharge values (200 m^3s^{-1}) resulted in a 9 day delay of the spring bloom due to high advection rates. (Figure 2.6).

2.3.6 Effect of Cloud Coverage

Interannual differences in cloud coverage has an insignificant effect on the timing of the spring bloom in Rivers Inlet. Cloud coverage is very consistant between years during the two months preceding the spring bloom (February and March). Average cloud coverage during February and March varies less than 10% between 2006-2010. The largest effect was seen using 2007 as the forcing cloud data. Using 2007 clouds resulted in a 3 day delay in the timing of the 2006 and 2009 spring bloom and a 1 day delay in bloom timing in 2008. All other years used to force cloud coverage resulted in an advance or delay of less than 3 days of the timing of the spring bloom.

2.3.7 Sensitivity to Biological Parameters

While only two biological parameters were used to tune the model($R_{max}(T_{ref})$ and Z_w), three parameters were examined to determine the effects on the timing of the spring bloom: maximum growth rate ($R_{max}(T_{ref})$), mortality ($R_M(T_{ref})$), and concentration of zooplankton (Z_w). The timing of the spring bloom is highly sensitive to growth rate and mortality and less so to concentration of zooplankton. Increasing the maximum growth rate from 2.16 to 2.8 day^{-1} (33%) results in a bloom that occurs 22 days earlier on av-

erage. Decreasing the mortality rate from 0.075 to 0.05 day^{-1} (33%) results in a bloom that occurs on average 7 days earlier. Decreasing the concentration of zooplankton from 0.089 to 0.06 (33%) results in a bloom that occurs on average 3 days earlier.

The spread of the spring bloom is defined as the time difference of the spring bloom between different years. Growth rate and mortality of phytoplankton have a larger effect on phytoplankton concentrations during the spring and summer months than during the winter. This results in changes in the spread of the spring bloom date when these parameters are varied. Increasing the maximum growth rate by 33% resulted in an average decrease in spread of 10 days while decreasing the mortality rate by 33% resulted in an average decrease in spread of 11 days. The zooplankton concentration has a constant effect on the winter and spring concentrations of phytoplankton. This results in zooplankton concentration not having a significant effect on the spread between the spring bloom dates. Growth rate and mortality of phytoplankton have a similar effect on the timing of the spring bloom thus only one parameter is needed for tuning the model. The mortality was set to 0.075day^{-1} at 10°C . A single value was found for each tuning parameter (Table 2.2) to produce optimal results for the timing of the spring bloom for the four years (Table 2.6).

2.4 Discussion

How do different physical forcings affect the timing of the spring bloom?

Wind speed and direction is the primary physical forcing on the timing of the spring bloom. In the winter months, strong winds increase the mixing layer depth (Figure 2.4), limiting phytoplankton growth (Figure 2.7). Increasing the mixing layer depth causes the phytoplankton to be mixed below their critical depth in which there is enough light to grow. Many large wind events are seen to decrease the depth averaged chlorophyll concentrations and wind speed and direction within the 2 months before the spring bloom have a significant impact on the timing of the spring bloom. The direction of large wind events can amplify the mixing layer depth. If the wind direction is directed down inlet towards the mouth, the fresh water layer is advected out of the fjord which is conducive to deeper mixing. Large wind events that are directed up inlet towards the head do not have this effect as the freshwater layer is not lost from the inlet. Outflow events will also result in flushing events that advect phytoplankton populations away from the basin.

A single outflow wind event within 2 weeks of the spring bloom caused a 7 day delay in the bloom timing.

Freshwater flux is a secondary control and has a large effect on the mixing layer depth as well as the timing of the spring bloom. Higher river flux increases the upwelling advection while shallowing the mixing layer depth. Low river discharge causes the opposite effect: less advection but a deeper mixing layer depth. Increased upwelling advection caused by high freshwater discharge is the dominant river effect in Rivers Inlet. In 2007, higher river input caused a muting effect on the mixing layer depth determined by wind events. However, the high river discharge in 2007 also resulted in all test years run with 2007 river data to experience a delayed bloom, illuminating the importance of advective loss of phytoplankton due to increased upwelling advection.

Interannual cloud coverage has an insignificant effect on the timing of the spring bloom in Rivers Inlet. Cloud coverage is very consistant between years in Rivers Inlet with an average of 80% cloud coverage in Feburary and March. Light is considered an important controller of phytoplankton biomass accumulation (Reynolds 2006) and is seen as a controlling factor in many locations including the Strait of Georgia (Collins et al. 2009) and northerly fjords in Norway (Eilertsen et al. 1995). If climatic changes were to effect the average winter and early spring cloud distribution over Rivers Inlet, cloud cover would have a much larger potential influence on the timing of the spring bloom.

Wind Driven Advection

Blooms in 2008 and 2009 occur 10 days apart due to differences in the wind direction of large wind events occurring within 6 weeks of the initiation of the bloom. Close examination of the winds in Rivers Inlet taken from the Laska and Ethel weather stations revealed 2 wind events in 2008 leading up to the bloom where the primary wind direction was up inlet (inflow), and in 2009, there was 1 very large wind event where the primary wind direction was down inlet, towards the mouth (outflow). Because of the high stratification seen in Rivers Inlet due to continual river input and the non-constricted opening at the mouth of the fjord, a large wind event directed down inlet causes rapid horizontal advection, flushing the phytoplankton population out of the inlet. The intensity of the flushing events is dependent on outflow wind timing and strength, strength of water column stratification, and how constricted the mouth opening is. Wind events large enough to reverse surface-layer flow were found to be a common occurrence in Knight Inlet

(Baker & Pond 1995). During 2-3 day wind forcings in Knight Inlet, speeds at 2m depth were as large as 30 cms^{-1} and up to 5 cms^{-1} as deep as 20-25 m. Incorporating an open basin system in the model resulted in an additional loss term of phytoplankton due to the advection from wind which produced significant effects on the timing of the spring bloom and explained the difference between the bloom timing in 2008 and 2009.

Single outflow wind events have significant effects on the timing of the spring bloom. Outflow wind events occurring within 2 months prior to the spring bloom caused a 4-7 day delay in the bloom timing. Events occurring in January and February had a smaller effect, shifting the bloom by 1-2 days. The shift in bloom timing resulting from multiple outflow wind events was greater than the sum of the individual wind events. The strength of the outflow event is of less importance than the timing. Doubling the strength of 1 outflow wind event 3 weeks before the spring bloom resulted in a 2 day delay in the timing of the spring bloom.

Significance

In the narrow valleys and fjords in British Columbia, significant winds will only occur as inflow or outflow (up or down valley) (Jackson & Steyn 1994). Outflow is the dominant direction in the winter (Jackson & Steyn 1992). Outflow winds, also known as gap or Squamish winds, occur when cold, dry air at low levels moves from the interior to the coast, dissecting the coastal mountains (Jackson 1993). Gap winds occur when a strong Arctic anticyclone develops a high pressure cold and stable air mass over the interior, east of the Coast Mountains. Differences in temperature and humidity between this air mass and the warm, moist coastal air, creates a large pressure gradient that is oriented perpendicular to the coast. This will cause strong low-level winds that develop in fjords and valleys. Strong outflow can also occur as a result of a deep cyclonic center that approaches the coast. This will create a similar pressure gradient, driving outflow winds through the fjords. These deep cyclonic centers produce frequent rainfall and southwesterly winds during the winter months in the Pacific Northwest (Logerwell et al. 2003). The timing of the transition between winter southwesterly winds and summer northeasterly winds is termed the spring transition. This transition can occur any time between March and June. (Logerwell et al. 2003, Thomson & Hourston 2009). In Rivers Inlet, large outflow events are not seen during summer months (Figure 2.7). Continuing north to Burke Channel, Cathedral Point, a weather station located near Bella Coola, BC also shows very large outflow wind events occurring

only in the winter months. Summer months (June - August) at Cathedral Point are indicative of smaller inflow wind events. While Rivers Inlet and Burke Channel both experience an increase in large out-flow events caused by large-scale low pressure systems during the winter months, the timing of such events is not correlated. Transition timing will effect all inlets along the coastline creating potential for outflow wind events, but the stochastic nature of these wind events will not allow a non-local generalization of outflow events along the British Colombia coast.

In fjord regions, the winds before the spring transition favor outflow within the fjord which cause a delay in the timing of the spring bloom. Logerwell et al. (2003) indexed the spring transition date for the Oregon Production Index (OPI) area based on the first day where the value of the 10-day running average for upwelling is positive and the 10-day running average for sea level is negative. Based on this index, the mean date of the spring transition occurs on April 6th but can range from early February to early July (Figure 2.8). Thomson & Hourston (2009) determine the spring transition timing off of the west coast of Vancouver Island using the alongshore wind stress at meteorological buoy 46206. The spring transitions showed strong similarities between the Oregon and British Colombia coastlines (Figure 2.8). One feature of note is the late transition dates that occur in the 1990's in both regions, with 2 years being the latest transitions seen since the 1970's. Late transition dates are more conducive to outflow winds occurring later in the spring which will delay the onset of the bloom.

It has been suggested that the timing of the spring bloom may be critical to the growth and survival of higher trophic levels (Cushing 1974, 1975, 1982, Richardson 2004, Ware & Thomson 2005). In the Strait of Georgia, early spring blooms can cause nauplii of *N. plumchrus* to miss the spring bloom causing them to rely solely on post-bloom phytoplankton which are less nutritious (El-Sabaawi et al. 2009). The sockeye salmon crash in Rivers Inlet occurred in the early 1990's, coinciding with the late transition dates seen off Vancouver Island. It has been hypothesized that bottom up effects control juvenile sockeye salmon growth in Rivers Inlet (Buchanan 2007). Changes in the Rivers Inlet spring phytoplankton bloom have caused interannual variability in the timing, magnitude and composition of the zooplankton bloom (Tommasi et al. 2010b). Match/mismatch of the phytoplankton bloom and the inlet zooplankton community may have resulted in less prey for juvenile salmon thus diminishing the success of recruitment and is a possible scenario leading to the decline of the sockeye salmon in Rivers Inlet.

Flushing events have potential to be an important controlling factor in determining the timing of the spring bloom. Flushing events have been seen

in Puget Sound (Winter et al. 1975) and in Otsuchi Bay, Japan (Furuya et al. 1993) where rapid horizontal advection caused the removal of plankton populations from the basins. However, in northerly Norway as well as high latitudes including West Spitzbergen the onset of the spring phytoplankton bloom is regulated by daylength and linked to the entrainment of phytoplankton resting spores from the bottom layers (Eilertsen et al. 1995) causing the spring phytoplankton bloom to occur at approximately the same time each year (Eilertsen et al. 1989). Rivers Inlet and Burke Channel display large outflow wind events leading up to the summer months. Sustained outflow winds will cause rapid horizontal flushing of the fjord causing a delay in the timing of the spring bloom. This suggests the importance of flushing events to spring bloom timing along the BC coast. Climatic changes in the large scale pressure systems encountering the BC coast would cause changes in the spring transition dates, potentially leading to more frequent and later occurring outflow events and ultimately delaying the timing of the spring phytoplankton bloom.

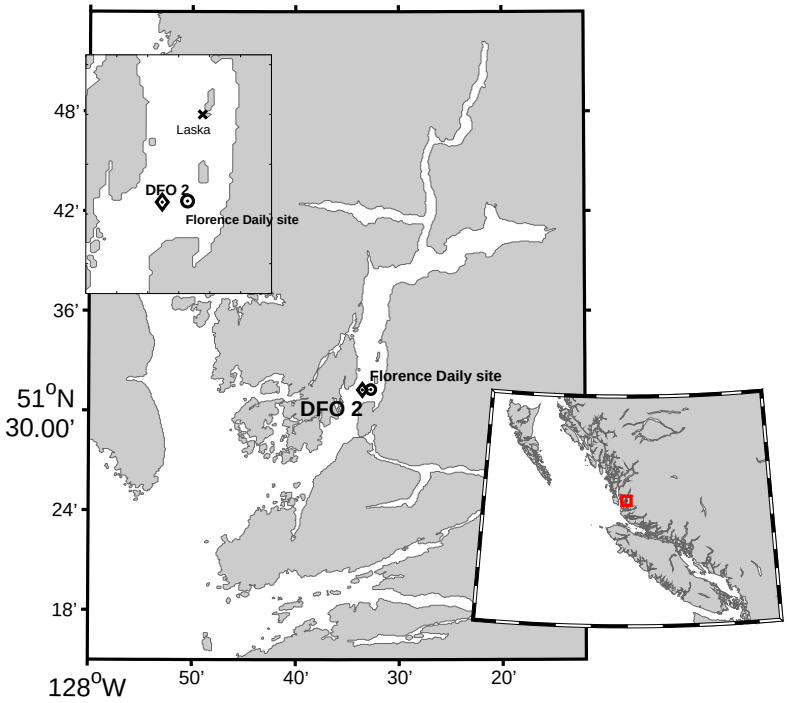

Figure 2.1: Map of Rivers Inlet on the West Coast of British Columbia including sample station DF02 (black diamond), the Florence Daily site (black circle) and the Laska meteorological station (black x).

Step 1	Step 2	Step 3	Step 4
$W_P < 50$	$W_P = W_P + 360$	Return to Step 1	
$W_P < 60$	$\lvert W_{PP} - W_P \rvert < 5$ $\mathbf{W_L = 360}$	$\lvert W_{PP} - W_P \rvert > 5$ $\mathbf{W_L = W_{LP}}$	
$W_P < 140$	$\mathbf{W_L = W_{LP}}$		
$W_P < 150$	$W_{LP} < 180$ $\mathbf{W_L = 180}$	$W_{LP} > 180$ $\mathbf{W_L = W_{LP}}$	
$W_P < 160$	$\mathbf{W_L = 180}$		
$W_P < 170$	$\mathbf{W_L = W_{LP}}$		
$W_P < 180$	$W_{LP} < 180$ $\mathbf{W_L = 360}$	$W_{LP} > 180$ $\mathbf{W_L = W_{LP}}$	
$W_P < 210$	$\mathbf{W_L = 360}$		
$W_P < 220$	$\lvert W_{PP} - W_P \rvert < 5$ $\mathbf{W_L = 360}$	$\lvert W_{PP} - W_P \rvert > 5$ & $W_{PP} < W_P$ $\mathbf{W_L = 180}$	$\lvert W_{PP} - W_P \rvert > 5$ & $W_{PP} > W_P$ $\mathbf{W_L = 360}$
$W_P < 240$	$\mathbf{W_L = 180}$		
$W_P < 260$	$\mathbf{W_L = W_{LP}}$		
$W_P < 280$	$\mathbf{W_L = 360}$		
$W_P < 300$	$\mathbf{W_L = W_{LP}}$		
$W_P < 310$	$\lvert W_{PP} - W_P \rvert < 5$ $\mathbf{W_L = W_{LP}}$	$\lvert W_{PP} - W_P \rvert > 5$ & $W_{PP} > W_P$ $\mathbf{W_L = 180}$	$\lvert W_{PP} - W_P \rvert > 5$ & $W_{PP} < W_P$ $\mathbf{W_L = 360}$
$W_P < 320$	$\lvert W_{PP} - W_P \rvert < 5$ $\mathbf{W_L = W_{LP}}$	$\lvert W_{PP} - W_P \rvert > 5$ & $W_{PP} > W_P$ $\mathbf{W_L = 180}$	$\lvert W_{PP} - W_P \rvert > 5$ & $W_{PP} < W_P$ $\mathbf{W_L = W_{LP}}$
$W_P < 390$	$\mathbf{W_L = 180}$		
$W_P > 390$	$\mathbf{W_L = W_{LP}}$		

Table 2.1: A regression tree developed to simulate the wind directions for Rivers Inlet using a comparison between the Port Hardy Airport and the Laska Meteorological Station wind directions. W_P is the current value of Port Hardy wind direction, W_{PP} is the previous value (1 hr. previous) of Port Hardy wind direction, W_L is the current value of Laska wind direction, and W_{LP} is the previous value (1 hr. previous)of Laska wind direction. Find the value of W_P being used in Step 1 and then continue on to Step 2 and continue following the steps until a value of W_L is reached.

Symbol	Parameter	Value	Source
$R_{max}(T_{ref})$	maximum growth rate (24hr)	2.16 day^{-1}	tuned, < Hitchcock (1980) > Durbin (1974)
T_{ref}	reference temperature	10°	
Pr_{th}	Predation threshold concentration	0.05	< Cugier et al. (2005)
$R_M(T_{ref})$	mortality	0.075 day^{-1}	< Spitz et al. (2003) > Denman & Peña (2002)
	maximum temperature for growth	18°	Durbin (1974)
	range of dec. due to temp.	8°	
κ_p	half-saturation for zooplankton grazing	0.2μM N	< Denman & Peña (2002)
$\Upsilon(T_{ref})$	maximum ingestion, mesozoo	0.6 day^{-1}	Cugier et al. (2005)
Z_w	zooplankton concentration	0.089μM N	tuned
	Chl/m^3 to μM N conversion	1.7:1	M. Maldonado, per. comm., February 9, 2010

Table 2.2: Model parameters used in the Biological Model. The '<' and '>' symbols indicate whether the value is greater than (>) or less than (<) the referenced value.

Run ID	Control Years	Forcing Varied	Value of Changed Forcing
R*wR6	R7,R8,R9	Wind	R6 wind
R*wR7	R6,R8,R9	Wind	R7 wind
R*wR8	R6,R7,R9	Wind	R8 wind
R*wR9	R6,R7,R8	Wind	R9 wind
R*rR6	R7,R8,R9	Freshwater	R6 freshwater
R*rR7	R6,R8,R9	Freshwater	R7 freshwater
R*rR8	R6,R7,R9	Freshwater	R8 freshwater
R*rR9	R6,R7,R8	Freshwater	R9 freshwater
R*cR6	R7,R8,R9	Clouds	R6 clouds
R*cR7	R6,R8,R9	Clouds	R7 clouds
R*cR8	R6,R7,R9	Clouds	R8 clouds
R*cR9	R6,R7,R8	Clouds	R9 clouds

Table 2.3: List of test runs to determine the impact of cloud coverage, wind, and freshwater on the timing of the spring bloom. List of the control runs is given in Table 2.6. The '*' in the Run ID is replaced by the number of the control run in column 2.

	R6	**R7**	**R8**	**R9**
R*wR6	0	-7	1	-2
R*wR7	10	0	6	3
R*wR8	-1	-11	0	-4
R*wR9	2	-6	3	0
R*rR6	0	-9	0	0
R*rR7	10	0	8	8
R*rR8	-1	-12	0	-1
R*rR9	0	-11	-1	0
R*cR6	0	-3	-1	0
R*cR7	3	0	1	3
R*cR8	1	-3	0	1
R*cR9	0	-2	0	0

Table 2.4: Table of results for test runs to determine the impact of cloud coverage, wind, and freshwater on the timing of the spring bloom. Numbers represent the number of days the bloom is advanced or delayed in comparison to the control run. Positive numbers are a delay in bloom date from the control run, and negative numbers indicate an earlier bloom, with 0 resulting in a same day bloom date. The '*' in column 1 is replaced by the number of the control run in columns 2-5. For example, the offset of bloom timing of R6wR7 is given in row 2, column 1 and is 10 days delayed from the control run.

Wind event label	Date of wind event	Average wind speed cubed
e1	Jan 2 - Jan 8, 2006	1569 m^3s^{-3} for 6 days
e2	Jan 31, 2006	702 m^3s^{-3} for 1 day
e3	Feb 28 - Mar 1, 2006	881 m^3s^{-3} for 3 days
e4	Apr 2, 2006	611 m^3s^{-3} for 1 day
e5	Apr 15 - Apr 19, 2006	591 m^3s^{-3} for 4 days

Wind event(s) reversed	Date of bloom
none (5 outflow events)	Apr 28, 2006
e3	Apr 24, 2006
e4	Apr 27, 2006
e5	Apr 21, 2006
e3,e5	Apr 17, 2006
e1,e3,e5	Apr 16, 2006
e2,e3,e5	Apr 16, 2006
all (5 inflow events)	Apr 9, 2006

Table 2.5: Using winds derived from Port Hardy, 5 outflow wind events were identified (e1, e2, e3, e4, and e5). A sensitivity test was done where a single wind event was reversed to an inflow event to determine the effect on the bloom timing. The upper table gives the labels of the outflow wind events that were identified, the date of the wind events, and the average wind speed cube of each wind event. The lower table gives the wind event(s) that were reversed to inflow event(s), and the resulting spring bloom date. Two examples: the first test run, was where all 5 wind events were outflow, resulting in a bloom that occurred on April 28th, 2006. The next test run reversed the e3 event to an inflow event, which resulted in a bloom that occurred on April 24th.

Run ID	Start Date	End Date	Observed Bloom	Modeled Bloom
R6	Sept 1 2005	Nov 1 2006	Mar 29-Apr 12 2006	Apr 9 2006*
R7	Oct 8 2006	Nov 1 2007	Apr 28th 2007	Apr 30 2007
R8	Aug 29 2007	Nov 1 2008	Apr 3th 2008	Mar 31 2008
R9	Sept 22 2008	Nov 1 2009	Apr 18th 2008	Apr 19 2008

Table 2.6: Model runs used to hindcast the spring blooms for 2006, 2007, 2008, and 2009 with the observed and modeled peak bloom dates. The modeled peak date for 2006 (*) uses modified wind directions as discussed in Section 2.3.4.

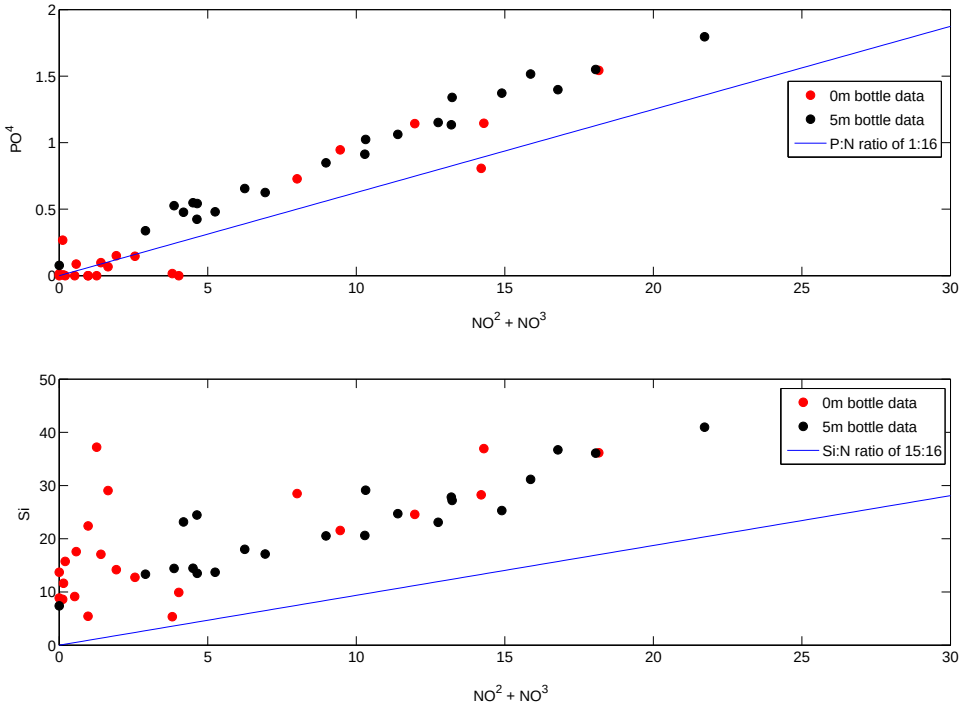

Figure 2.2: Nutrient limitation in Rivers Inlet: The ratio of PO^4 to NO^3 + NO^3 (a) and the ratio of Silica to NO^3 + NO^3 (b). Plotted is the 0m bottled data (red circles) and the 5m bottled data (black triangles) from the 2008 and 2009 fortnightly cruises at DF02. Nitrate is the limiting nutrient in Rivers Inlet.

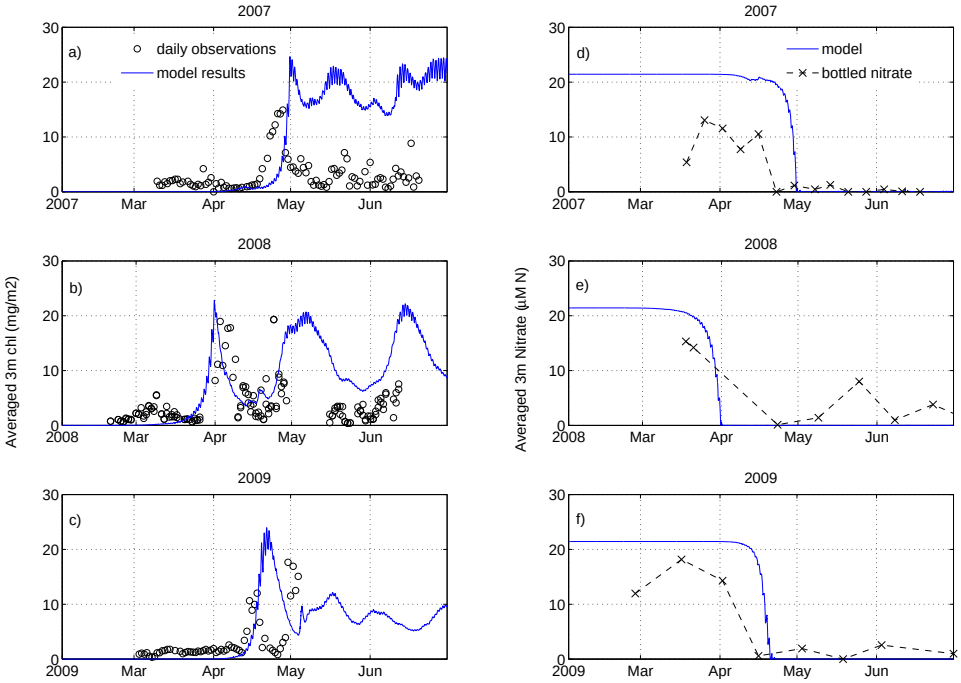

Figure 2.3: Modeled 0-3 m averaged phytoplankton (solid blue line) and observed daily 0-3 m averaged chlorophyll (black circles) for a) 2007, b) 2008, c) 2009. Surface modeled nitrate (solid blue line) and surface bottle sampled nitrate from bi-weekly cruises (x's connected by dashed black line) for d) 2007, e) 2008, f) 2009.

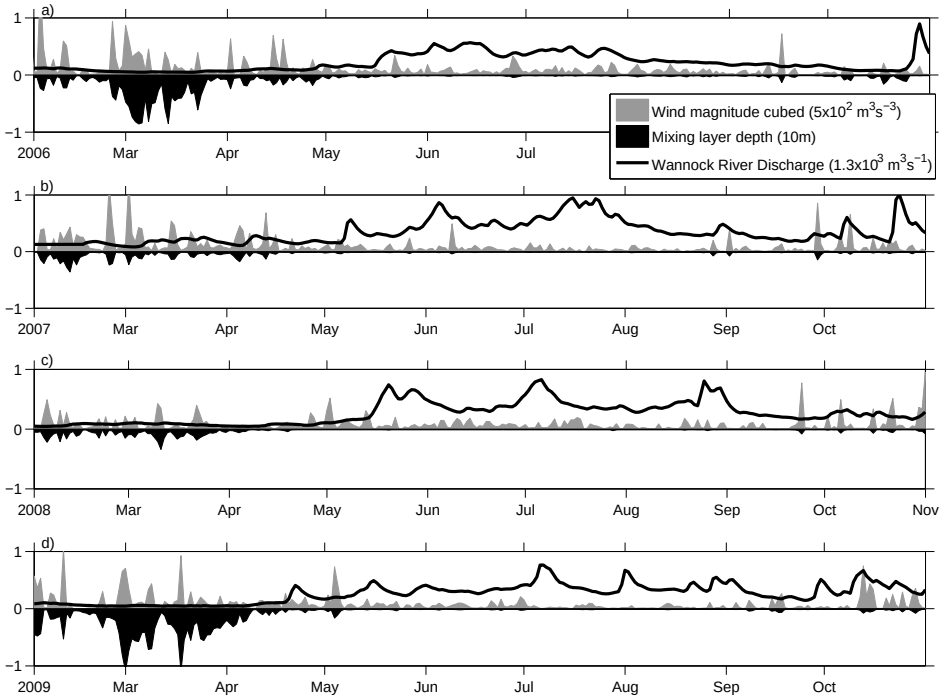

Figure 2.4: Daily-averaged wind speed cubed (gray shaded), modeled daily-averaged mixing layer depth(shaded black), and Wannock River flow (solid line) for February 1 to November 1 for each year. River flow in February-April was stronger in 2007 (226 m^3s^{-1}) compared with 2006 (95 m^3s^{-1}), 2008 (100 m^3s^{-1}) and 2009 (76 m^3s^{-1}) corresponding with a dampened mixing layer depth in 2007 (0.8 m from February-April). Stronger winds in 2006 (average windspeed cubed 97.31 m^3s^{-3}) resulted in a deeper mixing layer depth compared with 2008 (48.89 m^3s^{-3}), even though river input was similar. The mixing layer depth in 2009 was deepest (3.4m) due to low river input and several outflow wind events

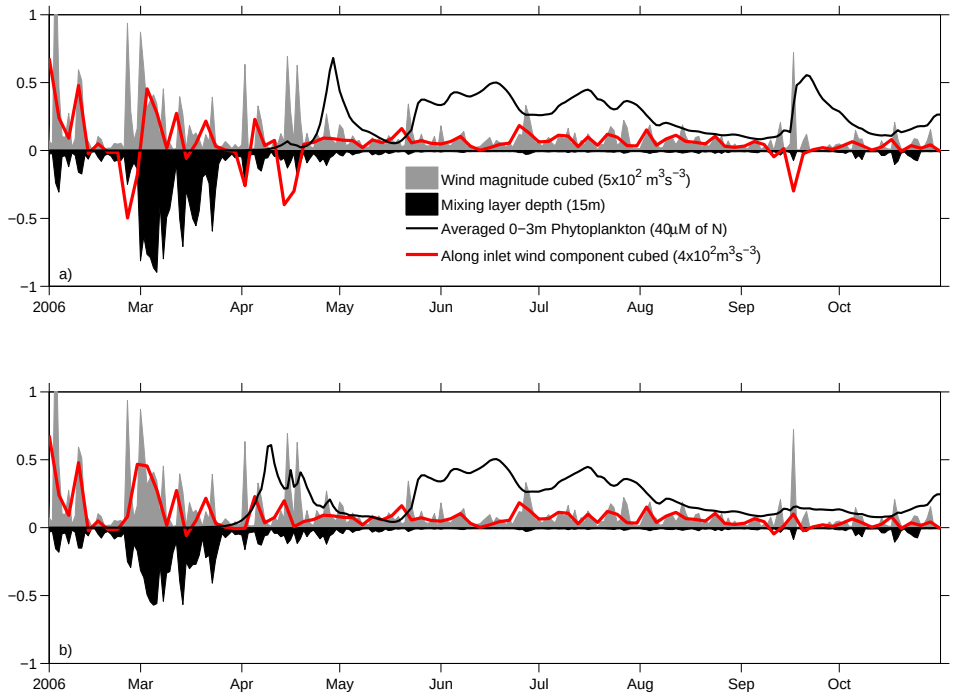

Figure 2.5: Daily-averaged wind speed cubed (gray shaded), modeled daily-averaged mixing layer depth (black shaded), modeled 0-3 m averaged phytoplankton (black line) and 3-day averaged along inlet wind component (red line) for (a) 2006 using winds derived from Port Hardy (b) 2006 where large outflow winds are reversed in direction (>400 m^3s^{-3}). Large outflow events occurring on March 24th and April 15th 2006 in the Port Hardy derived winds clearly affect the mixing layer depth.

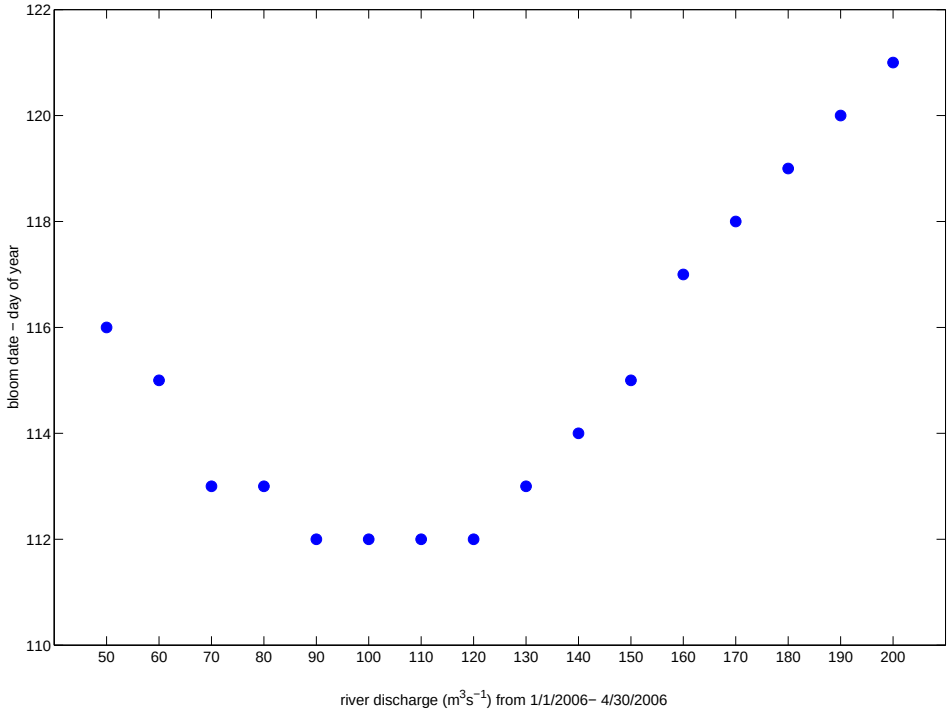

Figure 2.6: A sensitivity test to determine which river effect was dominant in Rivers Inlet. Large river discharge (200 m^3s^{-1}) results in higher upwelling advection leading to a larger advective loss term for phytoplankton, delaying the spring bloom. At low river discharge (50 m^3s^{-1}), the spring bloom is delayed due to a deeper mixing layer depth.

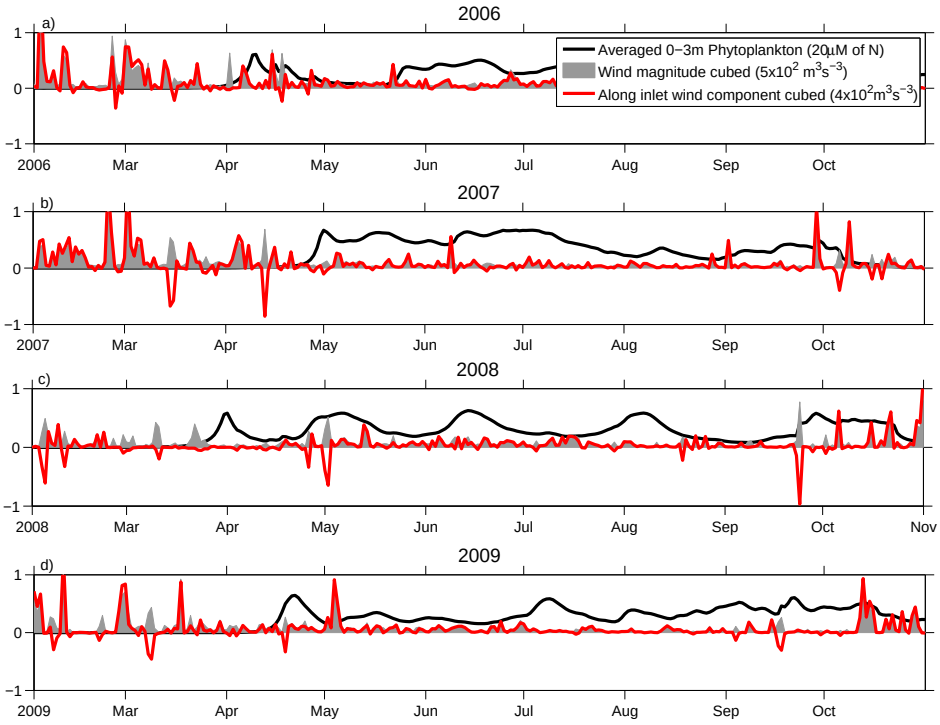

Figure 2.7: Daily averaged wind speed cubed (gray shading), modeled 0-3 m averaged phytoplankton (solid black line), and daily-averaged along inlet wind component (red line) for all four years. Winds are strongest in 2007 (Feb-April) (b) and weakest in 2008 (c); the bloom is latest in 2007 (b) and earliest in 2008 (c).

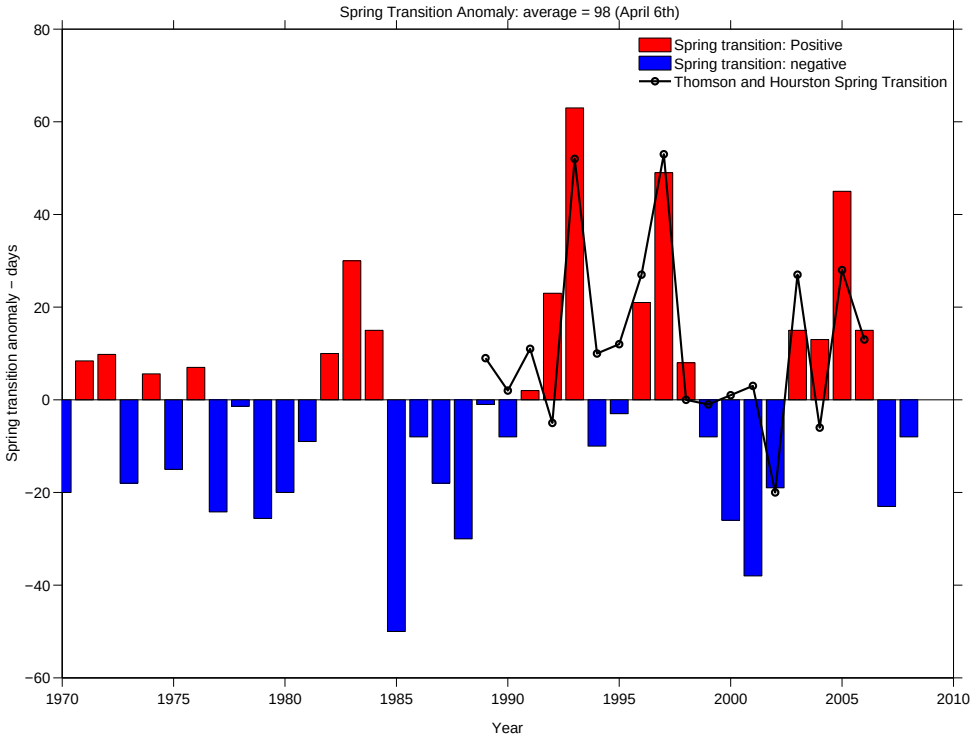

Figure 2.8: Anomalies in the date of the physical spring transition from 1969 to 2008 for the OPI area (shaded bars) and the spring transition dates for the west coast of Vancouver Island (Thomson & Hourston 2009). Anomalies are based on an average date of April 6th (Logerwell et al. 2003).

Chapter 3

Conclusions

The Rivers Inlet Ecosystem Study (RIES) set out to investigate the contribution of bottom up controls to the collapse of the Rivers Inlet sockeye salmon run. In the late 19th century, the Rivers Inlet fishery produced the 3rd largest catch of sockeye salmon in British Columbia (McKinnell et al. 2001) until a period of instability in the late 1970's and a large crash in the early 1990's reduced returns to only 1% of historic averages (Rutherford & Wood 2000, DFO 1997). Preliminary results indicate that reasons for the decline are due to an increased marine mortality rate of juvenile salmon (McKinnell et al. 2001). It has been hypothesized that increased cloud coverage, large wind events and higher river discharge in Rivers Inlet result in a delayed spring bloom and that sockeye survival rates are reduced due to bottom up controls on fish populations (Tommasi et al. 2010a).

This study examined the physical processes driving the timing of the spring phytoplankton bloom in Rivers Inlet using a coupled bio-physical model. Wind speed and direction, as well as freshwater inflow were found to control the timing of the spring bloom in Rivers Inlet. High wind speeds caused a deep mixing layer to occur which delayed the onset of the spring bloom. Large outflow wind events caused a flushing of the upper layer resulting in rapid horizontal advection of the phytoplankton population, delaying the bloom timing. River discharge has a significant yet complicated effect on the timing of the spring bloom. A sensitivity test exploring the effects of freshwater flux on bloom date was conducted using meteorological conditions from 2006. High river discharge averaging $200 m^3 s^{-1}$ between January and April stratified the water column, yet increased the upwelling advection resulting in a large advective loss term for phytoplankton. This resulted in a delay in the spring bloom timing. Low river discharge averaging $50 m^3 s^{-1}$ between January and April resulted in a deeper mixing layer depth due to reduced stratification which delayed the bloom as well. Thus both low and high river discharge result in a delay in bloom timing relative to moderate conditions. A moderate river discharge (in this case averaging $105 m^3 s^{-1}$) balances a high advection but shallow mixing layer with low advection but a deeper mixing layer. However, one should note that the

exact value of river flow giving the earliest spring bloom will depend on the specific meteorological conditions of a given year.

Observed interannual cloud coverage did not have a significant effect on the timing of the spring bloom. Cloud coverage is very consistent between years in Rivers Inlet in the 2 months prior to the spring bloom (February and March). If climatic changes were to affect the average winter and early spring cloud distribution, incoming light could have a much larger potential effect on the timing of the spring bloom in Rivers Inlet. This was in contrast to the Strait of Georgia which showed primary control of the spring bloom being driven by winds and a secondary control by incoming solar radiation with no significant changes caused by river influx (Collins et al. 2009). In the Strait of Georgia, advection is driven by freshwater flux which varies on the time scale of weeks, thus resulting in slow changes in vertical advection. Rivers Inlet is highly sensitive to freshwater discharge, with the residence time of the upper layer varying between 5-15 days (Hodal & Pawlowicz 2010). Fjords are characterized by significant buoyancy flux which can result in river discharge playing an important role in phytoplankton advective losses. Stratification of the water column also makes it possible for flushing events to occur during large outflow wind events.

Flushing events thus have potential to be a significant driving force determining the timing of the spring phytoplankton bloom. Rapid horizontal advection due to sustained winds has been seen in Puget Sound (Winter et al. 1975) and in Otsuchi Bay, Japan (Furuya et al. 1993) diluting the phytoplankton population. However, this is not true in many other fjord systems. Spring blooms occur at approximately the same time each year in northerly Norway as well as high latitudes including West Spitzbergen (Eilertsen et al. 1989). It has been suggested that the timing of spring blooms in northerly fjords is controlled by daylength and entrainment of phytoplankton resting spores from the bottom layers (Eilertsen et al. 1995). Our results suggest that the spring bloom in Rivers Inlet is largely affected by outflow winds which cause flushing events to occur. Wind data from Cathedral Point in Burke Channel, BC also displays large outflow events during the late winter, early spring months suggesting the importance of flushing events to spring bloom timing along the BC coast. The transition between winter southwesterly winds to summer northeasterly winds is termed the spring transition. Late spring transition dates are more conducive to outflow winds occurring later in the spring which produce flushing events that will delay the onset of the bloom. Climatic changes in the synoptic scale low pressure weather systems interacting with the BC coast could cause changes in the spring transition dates, thus leading to more frequent and later occurring

outflow events and ultimately delaying the timing of the spring phytoplankton bloom in fjords along the British Columbia coastline. Late transition dates will effect all inlets along the coastline creating potential for later occurring outflow wind events but due to the stochastic nature of these wind events, it is not predictable whether or not they will happen.

It has been hypothesized that the timing of the spring bloom may be influential to the survival of higher trophic levels (Cushing 1974, 1975, 1982, Richardson 2004, Ware & Thomson 2005). The relationship between the timing of plankton production, as a function of climate, to recruitment of fish has been coined by Cushing as the match/mismatch hypothesis (Cushing 1974, 1975). Temperature anomalies are one way in which climate variability may inhibit phytoplankton blooms, causing the bloom to occur either earlier or later than usual. Phytoplankton lead to a zooplankton bloom and will affect meroplankton (barnacle larvae). A mismatch can occur between primary producers and plankton, as well as between plankton and fish, resulting for example in less prey for juvenile fish larvae thus diminishing the success of recruitment (Cushing 1982). The correspondence of the sockeye salmon crash in Rivers Inlet with the late transition dates seen on Vancouver Island in the 1990's highlights the possible mechanism of outflow wind events causing delays in the timing of the spring bloom which could lead to a mismatch of the phytoplankton bloom and higher trophic levels. As to why Rivers Inlet experienced such a dramatic stock crash in comparison to other BC regions, Rivers Inlet may have had the right combination of outflow wind timing and strength, strength of water column stratification, and lack of inlet mouth constriction to focus the intensity of the flushing events creating the optimal conditions to delay the timing of the spring bloom enough to trigger a collapse in the higher trophic levels.

Rivers Inlet is one of many fjords located along the British Columbia coastline. While Rivers Inlet sockeye salmon stocks experienced an unprecedented collapse, corresponding declines have been seen in Northern and Central BC (McKinnell et al. 2001, Rutherford & Wood 2000, Riddell 2004). It is unknown whether the driving physical forcings examined in this study are controlling phytoplankton dynamics in these other regions. The bio-physical model used in this research to determine the environmental variables driving the spring bloom in Rivers Inlet could be expanded upon to establish the physical controls of the spring bloom in other systems, leading to insight on the decline in salmon survival along the BC coast. This study highlights the importance of precise wind speed and direction, which is specific to local regions. Accurate wind data is needed to correctly predict the timing of the spring bloom using the SOG bio-physical model. Meteo-

rological stations are needed in the areas of interest to acquire reliable wind information, in particular the months leading up to the spring bloom.

The primary objective of the RIES is to understand the dynamics of spring productivity and how it affects the growth of juvenile sockeye salmon. This study has clarified the driving physical controls on the timing of the spring bloom, and illustrated how large variations in the environmental variables can cause significant differences in the timing of the spring bloom. Fluctuations in environmental processes have been shown to influence changes in primary production and zooplankton abundance in Rivers Inlet (Tommasi et al. 2010a). Current research is being done on the seasonal and interannual dynamics of zooplankton, relating to variations in the physical environment and phytoplankton production and on the diet and growth rate of juvenile sockeye salmon in Rivers Inlet. This will help in our understanding of the mechanisms linking changes in the environment with productivity dynamics and growth to survival of juvenile sockeye salmon survival.

Bibliography

Baker, P. D., and S. Pond, 1995. Low-frequency residual circulation in Knight Inlet, British Columbia. J. Phys. Oceanogr., 25: 747-763.

Barber, R.T., and Chavez, F.P. 1983. Biological Consequences of El Niño. Science **222**(4629): 1203 – 1210.

Beamish, R.J., Noakes, D.J., McFarlane, G.A., Klyashtoria, L., Ivanov, V.V., and Kurashov, V., 1999. The regime concept and natural trends in the production of Pacific salmon. Can. J. Fish. Aquat. Sci.**56**(3): 516-526.

Buchanan, S.L., 2007. Factors influencing the early marine ecology of juvenile sockeye salmon (*Oncorhynchus nerka*) in Rivers Inlet, British Columbia. M.Sc. Thesis, Special Arrangements, Faculty of Science, Simon Fraser University, Burnaby, B.C.

Collins, A.K., Allen, S.E., and Pawlowicz, R., 2009. The role of wind in determining the timing of the spring bloom in the Strait of Georgia. Can. J. Fish. Aquat. Sci., **66**, 1597-1616.

Cugier, P., Menesguen, A., and Guillaud, J. F., 2005. Three-dimensional (3D) ecological modelling of the Bay of Seine (English Channel, France). J. Sea Res. **54**, 104-124.

Cushing, D.H., 1974. The natural regulation of fish populations. *In* Sea Fisheries Research *Edited by* F.R. Harden Jones. Elk Science, London. pp 399–412.

Cushing, D. H. 1975. Marine Ecology and Fisheries. Cambridge University Press, Cambridge.

Cushing, D. H. 1982. Climate and Fisheries. Academic Press, London.

Denman, K.L, and Peña, M.A, 2002. The response of two coupled one-dimensional mixed layer/ planktonic ecosystem models to climate change

in the NE subarctic Pacific Ocean. Deep-Sea Research Part II: 49: 4739-5757.

DFO, 1997. Rivers and Smith Inlet Sockeye. Department of Fisheries and Oceans Science stock status report D6-04, Department of Fisheries and Oceans, Ottawa.

Dickson, M.-L. and Wheeler, P. A., 1995. Nitrate uptake rates in a coastal upwelling regime: A comparison of pn-specific, absolute, and chl a-specific rates. Limnol. Oceanogr.**40**, 533-543.

Dobson, F.W., and Smith, S.D., 1988. Bulk models of solar radiation at sea. Quart. J. Roy. Met. Soc. **114**, 165-182.

Dyer, K.R. 1973. Estuaries: A Physical Introduction. Wiley-Interscience, New York and London, 70-71.

Durbin, E. G., 1974. Studies on the autecology of the marine diatom *Thalassiosira norden skioldii* cleve, 1. The influence of daylength, light intensity, and temperature on growth. J. Phycol. 10, 220-225.

Eilertsen, H.C., Taasen, J.P, Weslawski, J.M. 1989. Phytoplankton studies in the fjords of West Spitzbergen: physical environment and production in spring and summer. J. Plankton Res. **11**(6): 1245-1260.

Eilertsen, H.C, Sandberg, S., and Tøllefsen, H., 1995. Photoperiodic control of diatom spore growth: a theory to explain the onset of phytoplankton blooms. Mar. Ecol. Prog. Ser. **116**: 303-307.

Eilertsen, H.C. 1993. Spring blooms and stratification. Nature.**363**(24), doi:10.1038/363024a0.

El-Sabaawi, R.W., Kainz, M., Mazumder, Z., and Dower, J.F., 2009. Interannual variability in fatty acid composition of the copepod *Neocalanus plumchrus* (Marukawa) in the Strait of Georgia, British Columbia (Canada). Mar Ecol Prog Ser 382:151-161.

Erga, S. R., and Heimdal, B. R., 1984. Ecological studies on the phytoplankton of Korsfjor den, western Norway. The dynamics of a spring bloom seen in relation to hydrographical conditions and light regime. J. Plankton Res. 6, 67–90.

Environment Canada, 2009. Climate Database [online]. http://climate.weatheroffice.gc.ca/climateData/canada_e.html

Environment Canada, 2006. Hydrometric Data [online]. http://www.ec.gc.ca/rhc-wsc/.

Foerster, R.E, 1968. The sockeye salmon, *Oncorhynchus nerka*. Bull. Fish. Res. Board Can. 162. pp 422.

Foskett, D.R., 1958. The Rivers Inlet Sockeye Salmon. J. Fish. Res. Board of Canada. 15:867-889.

Frederiksen, M., Edwards, M., Richardson, A.J., Halliday, N.C., and Wanless, S., 2006. From plankton to top predators: bottom-up control of a marine food web across four trophic levels. J of Animal Ecology **75**(6): 1259-1268.

Furuya, K., Takahashi, K., and Iizumi, H., 1993. Wind-dependent formation of phytoplankton spring bloom in Otsuchi Bay, a ria in Sanriku, Japan. J. Oceanogr. **49**(4): 459-475.

Godfrey, H. 1958. A comparison of sockeye salmon catches at Rivers Inlet and Skeena River, B.C., with particular reference to age at maturity. J. Fish. Res. Board of Canada 15:331-354.

Hare, S.R., and Mantua, N.J., 2000. Empirical evidence for North Pacific regime-shifts in 1977 and 1989. Prog oceanogr. 47: 103-145.

Harrison, P.J., and Parsons, T.R.(Eds) 2000. Fisheries Oceanography: An Integrative Approach to Fisheries Ecology and Management. Blackwell Science, Oxford.

Hegseth, E.N., and Sakshaug, E., 1983. Seasonal variation in light and temperature dependent growth of marine planktonic diatoms in situ dialysis cultures in Trodheimsfjord, Norway(63^oN). J. Exp. Mar. Biol. Ecol. **67**, 188-220.

Hitchcock, G.L., 1980. Influence of temperature on the growth rate of *Skeltonema costatum* in response to variations in daily light intensity. Mar.Biol. **57**, 261-269.

Hodal, M., and Pawlowicz, R., 2010. Estimation of Net Physical Transports and Nutrient Fluxes for a Highly Stratified Coastal Fjord using Box Models: Applied to Rivers Inlet, British Columbia. Canadian Meteorological and Oceanographic Society Congress Abstracts, Ottawa, Canada. ID:3868.

Huisman, J., van Oostveen, P., and Weissing, F. J., 1999. Critical depth and critical turbulence: Two different mechanisms for the development of phytoplankton blooms. Limnol. Oceanogr. 44, 1781-1787.

Irigoien, X., Juisman, J., and Harris, R.P, 2004. Global biodiversity patterns of marine phytoplankton and zooplankton. Nature. **429**, 863-867.

Jackson, P.L., and D.G. Steyn, 1994. Gap winds in a fjord. Part I: Observations and numerical simulation. Mon. Wea. Rev. 122: 2645-2665.

Jackson, P., and Steyn D., 1992: The weather and climates of Howe Sound. Can. Tech. Rep. Fish. Aquat. Sci. 1789: 1-16.

Jackson, P. 1993: Gap winds in a fjord: Howe Sound, British Columbia. Ph. D. thesis. Department of Geography, University of British Columbia, Vancouver, BC.

Jerlov, N.G., 1976. Marine Optics volume 14 of Elsevier Oceanography Series. Elsevier Scientific Publishing Company, New York, New York, p 231.

Kaartvedt, S., and Svendsen, H., 1990. Advection of euphausiids in a Norwegian fjord system subject to altered freshwater input by hydro-electric power production. J. Plankton Research. **12**(6): 1263-1277.

Kelleher, K., and Weber, M.L., 2006. Toward Sustainable Management of World Fisheries and Aquaculture. *In* Global Issues for Global Citizens: An Introduction to Key Development Challenges. *Editied by* V.K Bhargava. Washington, DC: The World Bank. p. 285-304.

Lajus, J.A. 2004. Influence of weather and climate on fisheries: overview of emergence, approval and perception of the idea, 1850 –1950s. *In* International Commission on History of Meteorology. From Beaufort to Bjerknes and beyond: Critical Perspectives on the History of Meteorology; 2004 Jul 5-9; Polling Germany.

Lackey, R.T. 2009a. Challenges to sustaining diadromous fishes through 2100: lessons learned from western North America. *In* Challenges for Diadromous Fishes in a Dynamic Global Environment. *Edited by* A. Haro, K. L. Smith, R. A. Rulifson, C. M. Moffitt, R. J. Klauda, M. J. Dadswell, R. A. Cunjak, J. E. Cooper, K. L. Beal, and T. S. Avery. American Fisheries Society, Bethesda, MD, 609-617,

Lackey, R.T. 2009b. Salmon in Western North America: Historical Context. *In* Encyclopedia of Earth.*Edited by* C.J. Cleveland. Environmental Information Coalition, National Council for Science and the Environment, Washington, DC. Available from _http://www.dfo-mpo.gc.ca/CSAS/Csas/Publications/ResDocs-DocRech/2009/2009_022_e.htm_. [accessed 11 September 2009].

Large, W.G, J.C McWilliams, and Doney, S.C., 1994. Oceanic vertical mixing: A review and a model with a nonlocal boundary layer parameterization. Rev. Geophys. **34**(4): 363-403.

Large, W.G, and Pond, S., 1982. Sensible and latent heat flux measurements over the ocean. J. Phys. Oceanogr. **12**: 464-482.

Logerwell, E.A., Mantua, N.J., Lawson, P.W., Francis, R.C., and Agostini, V.N., 2003. Tracking environmental processes in the coastal zone for understanding and predicting Oregon coho (Oncorhynchus kisutch) marine survival. Fish. Oceanogr. **12**(6): 554-568.

Lavaniegos, B.E., Gomez-Gutierrez, J., Lara-Lara, J.R., Hernadez-Vazquez, S., 1998. Long- term changes in zooplankton volumes in the California Current System- the Baja California region. Mar Ecol Prog Ser 169: 55-64.

Leising, A.W., Gentleman, W.C., and Frost, B.W. 2003. The threshold feeding response of microzooplankton within Pacific high-nitrate low-chlorophyll ecosystem models under steady and variable iron input Deep-Sea Research Part II: Topical Studies in Oceanography, **50**(22-26): 2877-2894.

Longhurst, A. 1995. Seasonal cycles of pelagic production and consumption. Prog. Oceanogr. **36**(2): 77-167.

Lucas, L.V., Cloern, J.E., Koseff, J.R., Monismith, S.G., and Thompson, J.K. 1998. Does the Sverdrup critical depth model explain bloom dynamics in estuaries? J. Mar. Res. 56: 375-415.

Mann, K., and Lazier, J. 2006. Dynamics of marine ecosystems: Biological-physical interactions in the oceans. Blackwell Publishing, Malden, MA.

McKinnell, S.M, C.C Wood, D.T Rutherford, K.D Hyatt, and D.W Welch. 2001.The demise of Owikeno Lake sockeye salmon. North Americian J. of Fish. Mang. **21**(4): 774-791.

Ménesguen, A., Guillard, J. F., Aminot, A., and Hoch, T., 1995. Modeling the eutrophication process in a river plume - The Seine case-study (France). Ophelia 42, 206-225.

Mueter, F.J., Ware, D.M., and Peterman, R.M., 2002. Spatial correlation patterns in coastal environmental variables and survival rates of salmon in the north-east Pacific Ocean. Fish. Oceanogr. **11**(4): 205-218.

Noakes, D.J., Beamish, R.H., and Kent, M.L., 2000. On the decline of Pacific salmon and speculative links to salmon farming in British Columbia. Aquaculture **183**(3): 363-386.

Ottersen, G., Planque, B., Belgrano, A., Post, E., Reid, P.C., and Stenseth, N.C., 2001. Ecological effects of the North Atlantic Oscillation. Oecologia 128: 1-14.

Parsons, T.R., Takahashi, M., and Hargrave, B., 1984. Biological Oceanographic Processes. Pergamon Press, Oxford, p 330.

Pauley, G.B, Risher, G.B, and Thomas, G.L, 1989. Species Profiles: Life Histories and Environmental Requirements of Coastal Fishes and Invertebrates (Pacific Northwest) –Sockeye Salmon. U.S Fish and Wildlife Serv. Biol. Rep. 82(11.116).

Pedersen, F.B. 1978. A brief review of present theories of fjord dynamics, *In* Hydrodynamics of estuaries and fjords : proceedings of the 9th International Liege Colloquium on Ocean Hydrodynamics, 1977. *Edited by* Nihoul, J.C.J. Elsevier Oceanography Series, 23: pp. 407-422

Platt, T., Sathyendranath, S., and Fuentes-Yaco, C., 2007. Biological oceanography and fisheries management: persepective after 10 years. ICES Journal of Marine Science 64:863-869.

Reynolds, C. 2006. Ecology of phytoplankton. Cambridge University Press, Cambridge, UK.

Richardson, A.J. 2008. In hot water: zooplankton and climate change. ICES Journal of Marine Science 65: 279-295.

Richardson, A.J. 2004. Climate Impact on Plankton Ecosystems in the Northeast Atlantic. Science **305**(5690): 1609-1612.

Riddell, B. 2004. Pacific Salmon Resources in Central and North Coast British Columbia. Pacific Fisheries Resource Conservation Council. Vancouver, BC.

Rutherford, D.T., and Wood, C.C. 2000. Assesment of Rivers and Smith inlet sockeye salmon with commentary on small sockeye salmon stocks in Statistical Area 8. Fisheries and Oceans Canada, Canadian Stock Assessment Secretariat, Research Document 2000/162, Ottawa, Ontario.

Steele, J.H. 1962. Environmental control of phytosynthesis in the sea. Limnol. Oceanogr. **7**:137-150.

Spitz, Y.H., Newberger, P., and Allen, J.S., 2003. Ecosystem response to upwelling off the Oregon coast: Behavior of three nitrogen-based models. J. Geophys. Res. **108**, art. no. 3062.

Sverdrup, H.U. 1953. On conditions for the vernal blooming of phytoplankton. J. Conseil pour l'Exploration de la Mer. 18: 287-295.

Thomson, R., and Hourston, R., 2009. Winds, currents and temperatures. *In* State of physical, biological, and selected fishery resources of Pacific Canadian marine ecosystems. *Edited by* W.R Crawford and J.R. Irvine DFO Can. Sci. Advis. Sec. Res. Doc. 2009/022. pp 54-57. Avaiable from http://www.dfo-mpo.gc.ca/CSAS/Csas/Publications/ResDocs-DocRech/2009/2009_022_e.htm. [accessed 4 May 2010].

Tommasi, D. 2008. Seasonal and interannual variability of primary and secondary productivity in a coastal fjord. M.Sc Thesis, Department of Biological Sciences, Simon Fraser University, Burnaby, BC.

Tommasi, D., Routledge, R., Hunt, B., and Pakhomov, E., 2010a. Spring Phytoplankton Bloom Dynamics in a Fjord on the Central Coast of British Columbia. Can. J. Fish. Aquat. Sci., in press.

Tommasi, D., Routledge, R., Hunt, B., and Pakhomov, E., 2010b. Seasonal and interannual variability in zooplankton community structure in a fjord on the Central Coast of British Columbia, Can. J. Fish. Aquat. Sci., submitted.

Townsend, D. W, Keller, M. D., Sieracki, M. E., and Ackleson, S. G. 1992. Spring phytoplankton blooms in the absence of vertical water column stratification. Nature. **360**(6399): 59.

Valle-Levinson, A. 2010. Definition and classification of estuaries. *In* Contemporary Issues in Estuarine Physics. *Edited by* Valle-Levinson, A., Cambridge University Press, Cambridge, UK, pp. 1-11.

Ware, D.M., and Thomson R.E. 2005. Bottom-up ecosystem trophic dynamics determine fish production in the Northeast Pacific. Science 308(5626): 1280-1284.

Weijerman, M., Lindeboom, H., and Zuur, A.F., 2005. Regime shifts in marine ecosystems of the North Sea and Wadden Sea. Marine Ecology Progress Series 298: 21-39

Weitkamp, L. A., T. C. Wainwright, G. J. Bryant, G. B. Milner, D. J. Teel, R. G. Kope, R. S. Waples. 1995. Status review of coho salmon from Washington, Oregon, and California. U.S. Dept. of Commerce, NOAA Tech. Memo., NMFS-NWFSC-24, p. 258.

Welschmeyer, N.A., and Lorenzen, C.J., 1985. Chlorophyll budgets: Zooplankton grazing and phytoplankton growth in a temperate fjord and the Central Pacific Gyres. Limnol. Oceanogr. **30**(1), 1-21.

Wiafe, G., Yaqub, H.B., Mensah, M.A., and Frid, C.L.J., 2008. Impact of climate change on long- term zooplankton biomass in the upwelling region of the Gulf of Guinea. ICES Journal of Marine Science 65: 318-324.

Winter, D.F, Banse, K., and Anderson, G.C., 1975. The Dynamics of Phytoplankton Blooms in Puget Sound, a Fjord in the Northwestern United States. Marine Bio. **29**: 139-176.

Appendix A

Physical Model

The SOG model uses a version of the K-Profile Parametrization (KPP) non-local boundary layer model (Large et al. 1994) adapted to a coastal fjord region. The model reproduces the mixing due to turbulent vertical velocities of unresolved eddies and numerically calculates horizontal velocities, temperature, salinity, and diffusivities in both depth and time. To carefully determine the affects of surface mixing on phytoplankton growth in typical fjord density profiles, fine vertical resolution is needed. The SOG- model provides the needed vertical resolution of 0.25m to examine the near-surface mixing processes. Tides are neglected in this model. Tidal excursions are on the order of 3km in Rivers Inlet which is small in comparison to the length of Inlet basin.

The model procedure is as follows: the external forcings are prescribed, the diffusivity and non-local transport are calculated, and finally the mixing layer depth is determined.

The model is initialized with profiles of temperature (T), salinity (S) and chlorophyll fluorescence. Mixing at the surface is controlled by both turbulent and non-turbulent forcings. The turbulent forcings include wind stress, heat flux (including net long wave radiation, latent and sensitive fluxes) and freshwater flux. Non-turbulent forcing is determined using incoming solar radiation that is distributed over the water column. These forcings are applied continually using hourly meteorological data and daily river flow data. These external forcings are specific to Rivers Inlet and cause processes that vary horizontally (estuarine circulation, baroclinic pressure gradients) and must be parametrized into the model. The equations for across-inlet and along-inlet velocity, temperature and salinity are represented as:

$$\frac{\partial u}{\partial t} - fv = \underline{-\frac{1}{\rho_o}\frac{\partial p}{\partial x} - \frac{\partial}{\partial z}\left((w_e + w_w)u\right)} + V(u) \tag{A.1}$$

$$\frac{\partial v}{\partial t} + fu = \underline{-\frac{1}{\rho_o}\frac{\partial p}{\partial y} - \frac{\partial}{\partial z}\left((w_e + w_w)v\right)} + V(v) \tag{A.2}$$

$$\frac{\partial T}{\partial t} = \underline{-\frac{\partial}{\partial z}\left((w_e + w_w)T\right)} + \frac{I_{TOTAL}(z)}{c_p \rho(z)} + V(T) \tag{A.3}$$

$$\frac{\partial S}{\partial t} = \underline{-\frac{\partial}{\partial z}\left((w_e + w_w)S\right) - J_s \exp\left(\gamma z\right)} + V(S) \tag{A.4}$$

where u and v are the across and along inlet velocities, T is temperature, S is salinity, t is time, x, y are across and along inlet distance and z is zero at sea surface and positive upwards, f is the Coriolis parameter, V is the mixing prescribed by the KPP model (Large et al. 1994), ρ is the density of water, ρ_o is the constant reference density, p is the baroclinic pressure, c_p is the specific heat at constant pressure, w_e is a vertical estuarine-driven upwelling flux, w_w is the wind-driven vertical velocity, J_s is an added dilution rate, $1/\gamma$ is the scale depth of the freshwater flux and I_{TOTAL} is the incoming shortwave radiation. The additional terms added to the standard KPP model are underlined and are discussed in detail along with the incoming shortwave radiation in the *External Forcings* section.

External Forcings

The SOG model was originally optimized for the Strait of Georgia and included parametrizations for the specific physical dynamics of that basin. There were three components that were developed specifically for the Strait of Georgia that needed to be modified to model the physical behavior of Rivers Inlet. Firstly, freshwater input was modified. The influx of freshwater into the surface layer of Rivers Inlet causes it to remain relatively fresh, keeping the water column stratified and the vertical advection is assumed to be largely controlled by estuarine entrainment. Secondly, the parametrization of pressure gradients had to be changed to represent a narrower inlet. Finally, the light absorption scheme had to be re-parametrized to model the coastal light system of Rivers Inlet. These parametrization are discussed in greater detail in the following sections.

Freshwater flux

The physical dynamics in Rivers Inlet are primarily controlled by the river input of the Wannock River, driving the estuarine circulation.

Estuarine circulation has two effects which are seen in the salinity equation. First, the influx of freshwater into the surface layer of Rivers Inlet causes it to remain relatively fresh and keeps the water column stratified. Second, vertical advection is assumed to be largely controlled by estuarine entrainment.

Freshwater is added into the surface layer based on a parametrization of total freshwater flow into the Inlet. The surface salinity at DF02 is found

to be well correlated with the input of the Wannock River into Rivers Inlet. An empirical fit is determined for the surface salinity at station DF02 and is modeled as

$$S_{surface} = S_D \frac{\exp\left(-Q_W/\alpha_1\right) + \beta \exp\left(-Q_W/\alpha_2\right)}{\gamma_1 + \exp\left(-Q_W/\alpha_1\right) + \beta \exp\left(-Q_W/\alpha_2\right)} \tag{A.5}$$

where Q_W is the Wannock River flux, $S_D = 31.8$, $\alpha_1 = 80.0$ $\mathrm{m^3 s^{-1}}$, $\alpha_2 = 1500.0$ $\mathrm{m^3 s^{-1}}$, $\gamma_1 = 0.04$, $\beta = 0.01$. Figure A.1 shows the correlation between the surface salinity at DF02 and the river discharge from Wannock River. The empirical fit was forced to agree with physical requirements such that at low river discharge values, the surface salinity approached the bottom boundary salinity value of 31.8 and with very high river discharge, the surface salinity goes to zero (Figure A.1). This allows us to interpolate the observed salinities at DF02 to daily resolution. The surface salinities of the model are then forced to those of the observations using the following forcing term:

$$J_s \exp(\gamma z) = F_w Q_W S_o \left(\frac{Q_W}{\overline{Q}}\right)^{\sigma_s} \exp\left(\frac{z}{a_h h_m}\right) \tag{A.6}$$

where $F_w = 2.0\mathrm{x}10^{-6}\mathrm{s}^{-1}$, S_o is the mixed layer salinity at the previous time step, $a_h = 3.5$, $\overline{Q} = 7000\mathrm{m}^3\mathrm{s}^{-1}$, $\sigma_s = 1.38$, and h_m is the mixing layer depth determined by the KPP model. The scale depth over which the freshwater flux impacts the water column is $1/\gamma = a_h h_m$. The freshwater scale factor for river flow and the exponential on the amount of freshwater added to Rivers Inlet (F_w and σ_s in equation A.6, respectively) was tuned to give surface salinities that matched the empirical relationship (equation A.5). To determine a good match between model and observed halocline depths, the depth over which freshwater was added (a_h in equation A.6) was tuned. The dilution rate is proportional to the freshwater flux, Q_W which directly affects the stratification in the inlet (see equation A.4).

Estuarine entrainment is assumed to largely control upwelling and is parametrized into the model. The vertical velocity scale is determined using the Knudsen Relations, the vertical structure comes from the estuarine pressure gradient and turbulent momentum mixing (Collins et al. 2009). The empirical fit correlating upwelling velocity to river discharge is:

$$w_e = w_* \left[\frac{Q_W}{\overline{Q}} \exp\left(\frac{-Q_W}{\overline{Q}}\right)\right] \left[1 - \left(1 - \frac{z}{2.5d}\right)^2\right] \tag{A.7}$$

where $w_* = 1.08\mathrm{x}10^{-4}$ ms^{-1} and $d = 6.4$ m is the average depth at which the cumulative freshwater reaches 67% of its total value at DF02. The empirical

fit is forced to agree with physical requirements of zero vertical velocity at both zero river flow and infinite river flow. This vertical velocity controls the advection of temperature, salt, momentum, nitrate and phytoplankton. The vertical velocity is strongest at depth compared with the surface. This causes a convergence of water which results in a removal of these properties throughout the depth of the modeled water column. The observed upwelling velocities have a nearly linear relationship with river discharge at the values observed for the Wannock River (Figure A.2). This results in a higher advective loss term for phytoplankton due to an increase in freshwater discharge for all reasonable river flows.

Baroclinic Pressure Gradients

Due to the enclosed nature of Rivers Inlet, a flow in a given isopycnal layer will cause accumulation of a given layer downstream and a corresponding baroclinic pressure gradient against the flow. A parametrization of these pressure terms needed to be included in the model equations. Rivers Inlet is much narrower than the Strait of Georgia, causing the numerically calculated baroclinic velocities to produce high vertical mode numbers. This resulted in a step-like behavior in the density profiles that were not seen in observations. To compensate for this, we forced the model to mix implicitly by smoothing the diffusivity and increasing the interior viscosity.

Light

The physical model of SOG incorporates light in 4 parts: a standard calculation of total light to top of atmosphere based on solar angle and orbital geometry, a cloud model determining how much light is penetrating the atmosphere at a given time and hitting the water surface, an albedo (which controls how much light enters the water column), and the parametrization for the depth profiles of photosynthetically active radiation, I_{par}, and the total light spectrum that is available for heat, I_{total}(Collins et al. 2009).

The cloud model used in SOG, was developed following procedures developed for the North Atlantic Ocean (Dobson & Smith 1988). Short wave radiation was obtained from the Department of Agroecology Science at UBC (R. Ketler, personal communication, 2005). Cloud fraction data from the Vancouver International Airport was categorized using the okta system to parametrize the filtration of sunlight through the clouds, estimating the amount of light that penetrates the atmosphere at a given time and reaching the water surface (Collins et al. 2009).

The next parameter, albedo, is the fraction of light that is reflected back into the atmosphere after hitting the water surface. An albedo of 18% was calculated for the Strait of Georgia and was used as the value for Rivers Inlet. The total non-reflected light at the surface of the water column, $I_{total}(0m)$, is determined by the solar angle, the albedo, and the cloud filtering.

I_{par} must be distinguished from I_{total}. Comparison between the integration of the whole light spectrum at 0 m and between wavelengths 400-700 nm, reveals that 44% of the total light spectrum is within the range of 400-700 nm, in clear water (Jerlov 1976). In the SOG model, the biologically active surface irradiance value, $I_{par}(0m)$ is calculated as 44% of the total non-reflected light (I_{total}).

To determine a biologically active irradiance profile, a parametrization of light attenuation, K_{par}, is needed. Attenuation is the measure of how light is absorbed in the water column and is dependent on the amount of particular matter in the water. This includes organic material such as phytoplankton and inorganic material such as sediments transported by the river. Examination of I_{par} profiles taken at the daily station from February - June 2009 showed a positive correlation between the attenuation coefficient and with the amount of phytoplankton biomass in the water column (based on chlorophyll concentrations) and no significant correlation with the amount of river discharge. Data from other years was either unavailable or unrealistically dark. An empirical fit of the change in I_{par} over depth, eK, was determined where $eK = \exp(-K_{par}dz)$ is a function of depth with $dz = 1$m. An empirical relationship between the measured light and the phytoplankton quantity in the water (measured chlorophyll, P_c) was found to be:

$$K_{par} = \alpha_l + \beta_l \bar{P}^{0.665} + \theta_l \exp\left(\frac{z}{d_l}\right) \tag{A.8}$$

where $\overline{P} = P_c/(1\text{mg Chl } m^{-3})$ and the exponent on $\overline{P}$ follows Ménesguen et al. (1995). The empirical fit gave $\alpha_l = 0.1709$ m^{-1}, $\beta_l = 0.02$ m^{-1}, $\theta_l = 2.53$ m^{-1}, and $d_l = 0.53$ m. Figure A.3 compares real eK profiles calculated using daily I_{par} profiles from 2009 with the empirical eK profiles determined using equation A.8.

The total distribution of light in the water column used to calculate the non-turbulent heat flux profile is taken from the Jerlov (1976) water classification system providing data on the distribution of light with depth. This distribution follows a double exponential decay. Collins et al. (2009) discusses the two attenuation coefficients estimated for each water type. Total light is determined by integrating from the surface.

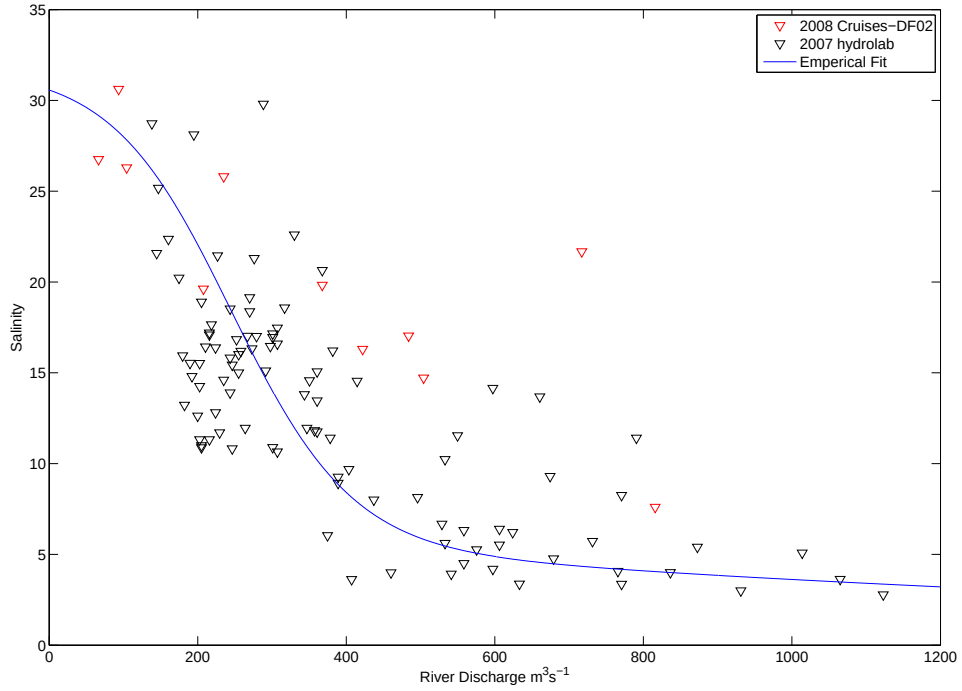

Figure A.1: Daily surface salinity values at DF02 from 2007 using the Hydrolab®DS5X sonde (black triangles), measurements taken during the 2008 bi-weekly cruises (red triangles) and the empirical fit determined to correlate surface salinity at DF02 and Wannock River discharge (blue solid line)

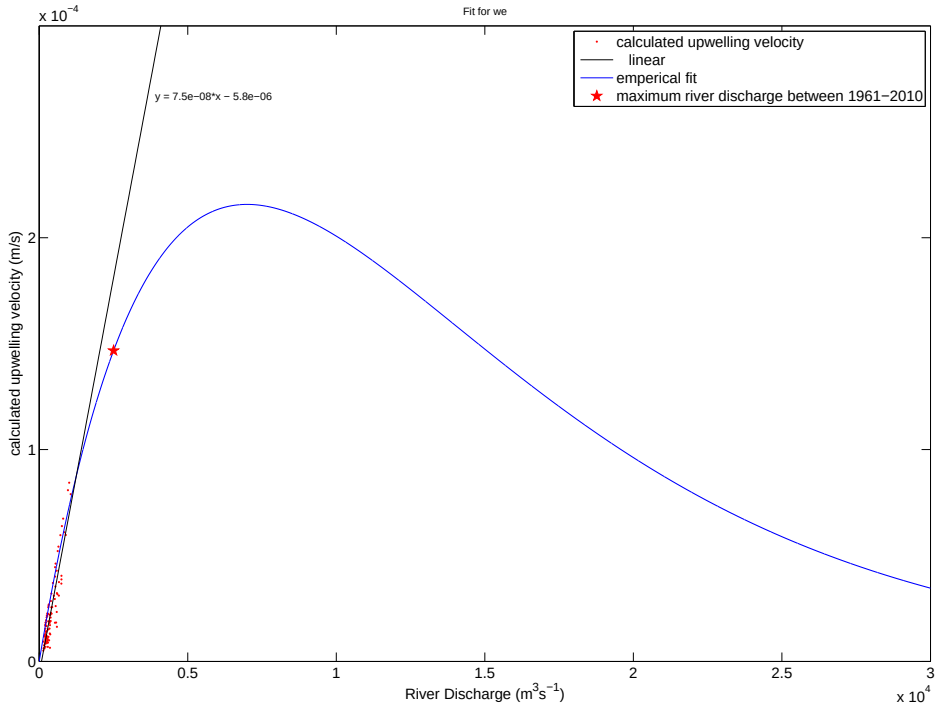

Figure A.2: The observed upwelling velocities (red dots), the linear fit to the data (black line), the empirical fit using equation A.7 (blue line), and the largest river discharge observed in the Wannock River between 1961-2010 (red star).

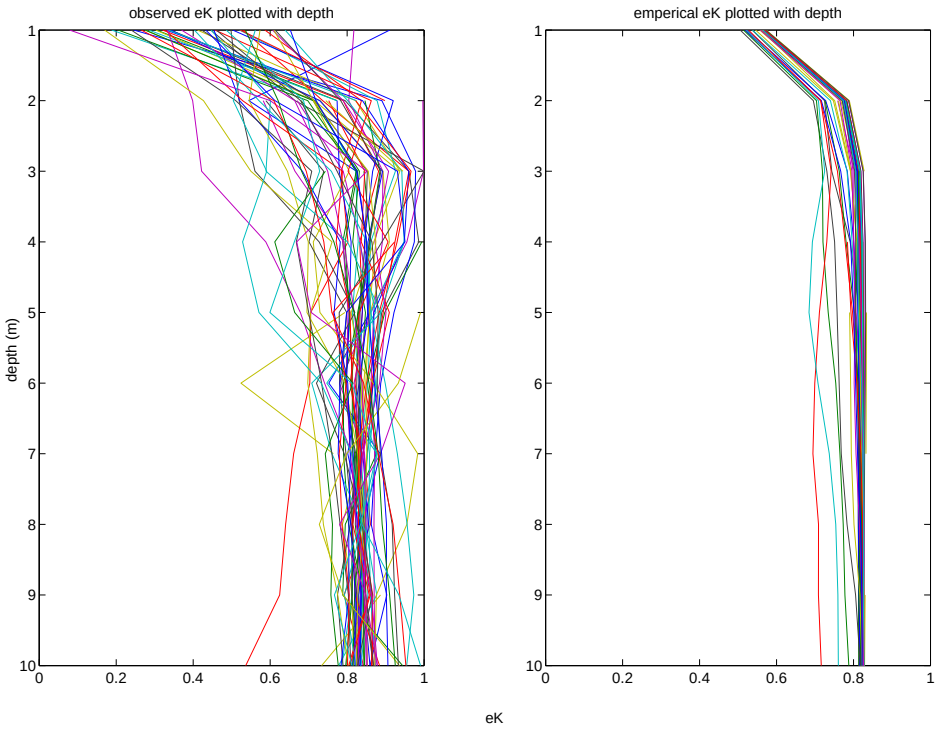

Figure A.3: a) Observed eK profiles from the daily 2009 I_{par} profiles and b) modelled eK profiles using equation A.8.

Appendix B

Biological Model

The biological model used in SOG is a simplified NPZ model (Collins et al. 2009). The biological model is a nitrogen model, where all units are nitrogen atom concentrations. The phytoplankton and nitrate equations used in the model are

$$\frac{\partial P}{\partial t} = \{\min[u_c(I_{PAR}), u_n(N)] - R_m\}P - \Upsilon\frac{Z(t,z)(P - Pr_{th})}{\kappa_P + P - Pr_{th}} + \frac{\delta}{\delta z}(w_s P) - \frac{\delta}{\delta z}((w_e + w_w)P) + V(P) \tag{B.1}$$

$$\frac{\partial N}{\partial t} = \{\min[u_c(I_{PAR}), u_n(N_0)]\}P - \frac{\delta}{\delta z}((w_e + w_w)N) + V(N) \tag{B.2}$$

where P is the phytoplankton concentration, N is the nitrate concentration, Pr_{th} is threshold concentration for feeding on P, u_c is the growth based on light-limitation, u_n is the growth due to nitrate limitation, R_m is the rate of natural mortality, Z is the zooplankton concentration, Υ is the maximum ingestion of phytoplankton by zooplankton, κ_p is the half-saturation for zooplankton grazing, w_s is the sinking rate of phytoplankton and the last two terms of each equation are the estuarine advective loss and turbulent diffusion calculated by the physical model (Appendix A).

The spring bloom is initiated as light limitation is lifted and is terminated by nitrate exhaustion. The first organisms to bloom are diatoms. In 2007, the bloom contained both *Skeletonema costatum* and *Thalassiosira* spp., while in 2008 the bloom was dominated by *Thalassiosira* spp (Tommasi et al. 2010a). Our model is thus limited to one nutrient type (nitrate) and one phytoplankton class (diatoms). The growth rate of phytoplankton and the temperature dependency is based on *Thalassiosira* spp.. Both *Skeletonema costatum* and *Thalassiosira* spp. have high growth rates at low light and low temperatures and can dominate the bloom early in the season (Hegseth & Sakshaug 1983). *Skeletonema costatum* can tolerate a wide temperature and salinity range unlike *Thalassiosira gravida* which has a much narrower range of comfortable temperatures and is most competitive below 10^oC (Hegseth & Sakshaug 1983). Modeling *Skeletonema costatum* instead of *Thalassiosira* would cause an insignificant difference in finding the timing of the spring bloom because both diatoms have high growth rates at low

light and low temperatures. If the timing of a summer bloom was of interest, the growth rate temperature dependace of the different species would become an important factor that would have to be taken into consideration.

Initialization

The biological model is initialized using two profiles: a profile of chlorophyll fluorescence measurements to initialize the phytoplankton and sample nitrate bottle data to initialize nitrate concentrations. Fluorescence measurements are converted from mg Chl/m^3 to μM N using a conversion factor 1.7:1 (M. Maldonado, personal communication, February 9, 2010). Bottle data was sampled at 0, 5, 10, 30 and 50m and is interpolated on 0.25m intervals matching the grid spacing of the physical model. Nitrate concentrations were considered constant between 40-50m which is consistent with observations seen at multiple stations throughout Rivers Inlet.

Phytoplankton Growth

Growth of phytoplankton is limited by both light and nitrate. The limiting factor is determined by whichever is a minimum. If there is an abundance of nitrate, growth rates will be dependent on the amount of light available

$$u_c = R_{max}(T)\left[1 - \exp\left(\frac{-I_{PAR}}{0.67I_{opt}}\right)\right]\left[1.8\exp\left(\frac{-I_{PAR}}{2.7I_{opt}}\right)\right] \tag{B.3}$$

where $I_{opt} = 38.4$ W/m^2 is the light intensity for peak growth and $R_{max}(T)$ is the maximum growth rate and was tuned to 2.16 day^{-1}. The maximum growth value for *Thalassiosira nordenskioldii* was measured by Hitchcock (1980) and Durbin (1974) as 2.8 day^{-1} and 2.0 day^{-1}, respectively. The maximum growth value is not known in Rivers Inlet but the value used in the model is between these values. The coefficients are chosen to give a Steeles-like shape for low light (Steele 1962, Collins et al. 2009) and to fit experimental light curves for *Thalassiosira* spp. (Collins et al. 2009). The relationship between photosynthetic growth rate and light intensity described by equation B.3 is shown in Figure B.1. Respiration is incorporated in the model as part of the natural mortality term.

When light availability is not limiting, growth rates depend on nitrate availability

$$u_n = R_{max}(T)\frac{N}{\kappa + N} \tag{B.4}$$

where $\kappa = 0.5\mu$M is the half-saturation constant for nitrate (N) (Collins et al. 2009).

Mortality and Grazing

Phytoplankton loss terms include natural mortality and grazing. Morality ($R_m(T)$) is taken as 0.075 day^{-1}at $10°C$ (between values used by Spitz et al. 2003 and Denman & Peña 2002). Grazing is based on a tuned zooplankton concentration that is held constant throughout the year. Winter concentrations of zooplankton are similar between years. Zooplankton concentrations do not increase significantly until after the spring phytoplankton bloom occurs (Tommasi et al. 2010a). This results in an insignificant effect of a grazing curve on the timing of the spring bloom, allowing for a constant zooplankton concentration to be used in the model.

A density-dependent mortality rate was used to described the functional response of zooplankton grazing at very low chlorophyll levels. The grazing threshold is defined as the concentration of prey, below which, the predator stops feeding (Cugier et al. 2005, Leising et al. 2003). A value of 0.09 mg Chlm^{-3} was used for the chlorophyll predation threshold.

Sinking

The sinking rate of diatoms increases when they are nutrient limited (Cugier et al. 2005). Nutrient limitation is calculated following Cugier et al. (2005).

$$f_N = \frac{N}{\kappa + N} \tag{B.5}$$

and the sinking speed as

$$w_s = W_1 f_N^{0.2} + W_2 \left(1 - f_N^{0.2}\right) \tag{B.6}$$

where $W_1 = 0.5$ m·day^{-1} and $W_2 = 1.2$ m·day^{-1} are the sinking rates for nutrient rich and nutrient depleted diatoms, respectively.

Temperature Dependency

There is a temperature dependency that is implemented in the model for maximum growth rate, grazing and mortality by multiplying each by

$$\exp\left[\alpha_T \left(T - T_{ref}\right)\right] \tag{B.7}$$

where $T_{ref} = 10^o$C, $\alpha_T = 0.07^o\text{C}^{-1}$ and T is the modeled temperature. This temperature effect is computed at all model depths.

An additional temperature effect is applied on the phytoplankton growth rate. *Thalassiosira nordenskioldii* is not observed to grow above 18°C (Durbin 1974). The growth rate was multiplied by a linear decrease from 1 to zero as the temperature increases from 10°C to 18°C (Collins et al. 2009).

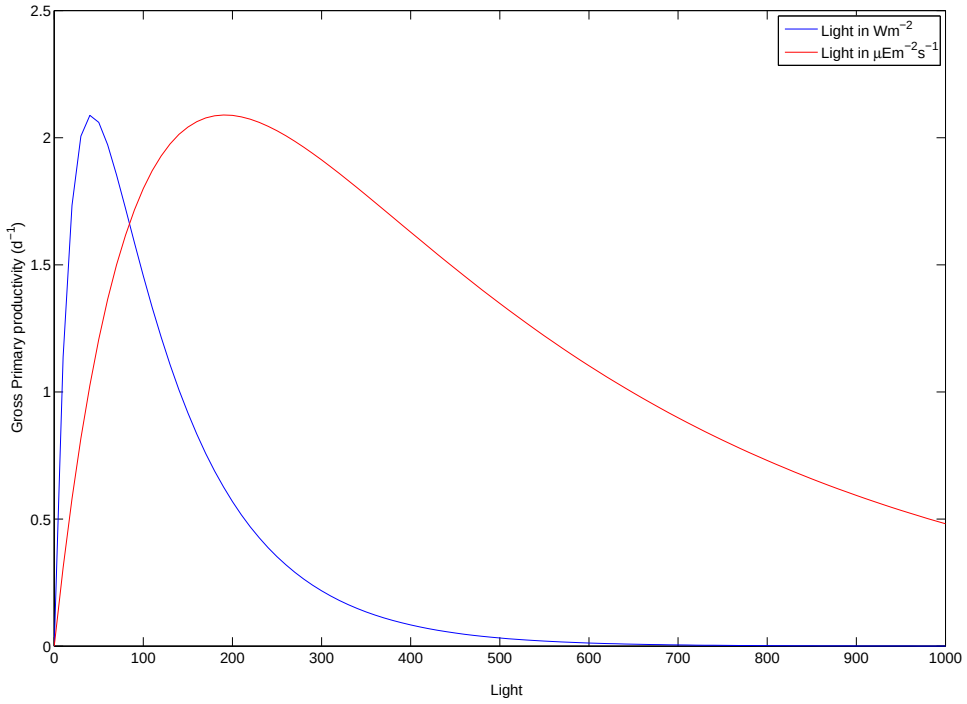

Figure B.1: The relationship between photosynthetic growth rate and light intensity described by equation B.3 in Wm^{-2} (blue line) and in $\mu\mathrm{Em}^{-2}\mathrm{s}^{-1}$ (red line).

Appendix C

Wind-driven Vertical Advection

For a semi-enclosed basin, such as the Strait of Georgia, the SOG code considers the basin to be a closed ellipse. The amount of water at each level moving in each direction is integrated and the thickening/thinning of the isopycnal layers is calculated (Collins et al. 2009). Baroclinic pressure gradients are calculated and this allows rotationally modified internal seiching to occur in basin.

In a fjord, such as Rivers Inlet, flows are predominately along axis. Flow toward the head of the inlet acts much like the flow in the closed basin described above. However, surface flow out of the inlet will leave the inlet and not cause back pressure gradients. This upper layer is lost to the inlet and deeper water moves upward. The background estuarine circulation is calculated separately. The strong surface flows considered here are primarily driven by the wind. Outward flows driven by the wind were observed to penetrate to about 15 m depth in a nearby fjord (Baker & Pond 1995). We use this depth to separate flow that easily leaves the fjord from deeper return-type flows.

For each depth-point in the model, the height of that isopycnal at each of the four directions east, west, north and south which run across and along the axis of the eclipse is tracked. The density field at the east, west, north and south extremes of the basin are integrated to calculate the baroclinic pressure field.At each step, the vertical mean is removed from the newly calculated velocities from the KPP mixing model to give the baroclinic currents. These velocities are added to time-integrated velocities along and across the fjord. For all directions, except the open end, the updated isopycnal distortions are calculated simply based on the time-integrated velocities (Collins et al. 2009).

For the open end, the isopycnals, above the depth of 15 m, are not allowed to tip downward. If the flow is outward in the surface layer, the isopycnals toward the mouth will be limited whereas those toward the head will not be. Thus these isopycnals will not be straight but kinked (Figure C.1). If

the velocity above the kinked isopycnal is outward toward the mouth of the inlet, a vertical velocity at the center point is calculated as:

$$w_w = \int_0^{bot} \frac{v\kappa}{Ly/2}(-dz) \tag{C.1}$$

where $bot = 40$m is the bottom of the model and v is the outward velocity if the velocity is outward and zero otherwise. As a last step, the integrated velocity in each layer is adjusted to conserve mass given the divergence in the vertical flow.

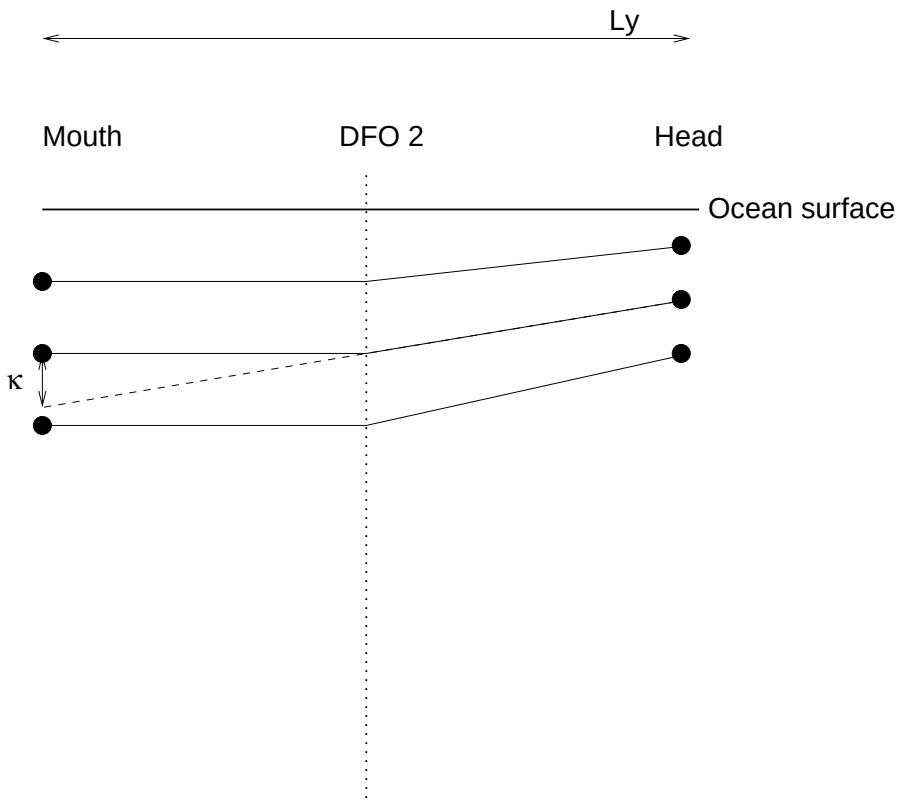

Figure C.1: Sketch showing the upper part of the model water column during outward surface flow. The black circles show the calculated isopycnal positions at the head and mouth of the fjord. Solid lines connect them. The dotted line shows the extension of the isopycnal tilt and the definition of the kink, κ.